

CAMS confirmation of previously reported meteor showers



P. Jenniskens^{a,b,*}, Q. Nénon^a, P.S. Gural^c, J. Albers^a, B. Haberman^a, B. Johnson^a, D. Holman^a, R. Morales^d, B.J. Grigsby^{a,e}, D. Samuels^d, C. Johannink^f

^aSETI Institute, Carl Sagan Center, 189 Bernardo Avenue, Mountain View, CA 94043, USA

^bNASA Ames Research Center, Mail Stop 241-11, Moffett Field, CA 94035, USA

^cLeidos, 14668 Lee Road, Chantilly, VA 20151, USA

^dFremont Peak Observatory Association, P.O. Box 1376, San Juan Bautista, CA 95045, USA

^eLick Observatory, U.C. Santa Cruz, 7281 Mount Hamilton Road, CA 95140, USA

^fDutch Meteor Society, Schiefestrasse 36, D 48599 Gronau, Germany

ARTICLE INFO

Article history:

Received 18 May 2015

Revised 1 July 2015

Accepted 8 August 2015

Available online 14 August 2015

Keywords:

Meteors

Comets, dust

Interplanetary dust

Near-Earth objects

Asteroids

ABSTRACT

Leading up to the 2015 IAU General Assembly, the International Astronomical Union's Working List of Meteor Showers included 486 unconfirmed showers, showers that are not certain to exist. If confirmed, each shower would provide a record of past comet or asteroid activity. Now, we report that 41 of these are detected in the *Cameras for Allsky Meteor Surveillance* (CAMS) video-based meteor shower survey. They manifest as meteoroids arriving at Earth from a similar direction and orbit, after removing the daily radiant drift due to Earth's motion around the Sun. These showers do exist and, therefore, can be moved to the IAU List of Established Meteor Showers. This adds to 31 previously confirmed showers from CAMS data. For each shower, finding charts are presented based on 230,000 meteors observed up to March of 2015, calculated by re-projecting the drift-corrected Sun-centered ecliptic coordinates into more familiar equatorial coordinates. Showers that are not detected, but should have, and duplicate showers that project to the same Sun-centered ecliptic coordinates, are recommended for removal from the Working List.

© 2015 Elsevier Inc. All rights reserved.

1. Introduction

The IAU Meteor Data Center maintains a list of all meteor showers discussed in the recent literature. This Working List of Meteor Showers contains 581 showers per May 2014, of which only 95 are “established”, meaning showers that are certain to exist. That leaves 486 unconfirmed showers (Jopek and Kanuchová, 2014).

Showers up to #88 were identified from photographed orbits obtained in the Harvard Super-Schmidt program (Jacchia et al., 1961; Southworth and Hawkins, 1963; Cook et al., 1972). Twenty-seven have now been confirmed, but others remain in doubt.

Showers with numbers up to #318 are from the Working List by Jenniskens (2006), which is based on streams identified from either the Harvard Radio Meteor Project derived orbits (Sekanina, 1973, 1976), from small numbers of photographed orbits, or in some cases only from visual observations. Thirty-eight have been established, but some of these are missing even measured orbital elements (Jopek and Kanuchová, 2014). For this list, lack of

confirmation is probably on account of the original pairings not being statistically significant. Hence, non-detection can be cause for removing these showers from the Working List.

Showers up to #408 are mostly from the Canadian Meteor Orbit Radar (CMOR) meteoroid orbit survey (Brown et al., 2008a, 2008b, 2010). Twenty-six have been established, including nearly all from the first batch of showers published (#319–332). Most showers from the second batch still need confirmation. This radar is sensitive to faint meteors in the +6 to +8 magnitude range, especially with entry speeds of 20–40 km/s. In this case, non-detection in video-based surveys does not rule out that the shower does exist.

The recently added Working List entries with numbers 409–623 are mostly from low-light video camera networks, and include single-station derived data. The largest multi-station study is that of the SonotaCo consortium, which captured over 168,000 meteors in the period 2007–2013 (Kanamori, 2009). Ongoing video surveys include that of the single-station IMO Video Network, with an annual yield of 350,000+ apparent trajectories (Molau and Arlt, 1997; Molau and Rendtel, 2009; Molau et al., 2013; Molau and Barentsen, 2014), the 80,000+ orbits in the EDMOND database (Kornos et al., 2012, 2014; Koukal et al., 2014), and the 19,055 meteoroid orbits collected in the period 2007–2010 by the

* Corresponding author at: SETI Institute, 189 Bernardo Ave, Mountain View, CA 94043, USA. Fax: +1 650 962 9419.

E-mail address: Petrus.M.Jenniskens@nasa.gov (P. Jenniskens).

Croatian Meteor Network (Vida et al., 2012; Korlevic et al., 2013; Segon et al., 2014a,b,c; Gural et al., 2014; Andreic et al., 2014a,b).

The *Cameras for Allsky Meteor Surveillance* (CAMS) project was conceived to validate as many as possible of the unconfirmed showers by scaling up video-based meteor triangulation. A network of 60 video cameras at three stations in California has measured trajectories of +4 to -1 magnitude meteors, and calculated their pre-atmospheric orbits since October of 2010 (Jenniskens et al., 2011). A second network is being developed in the BeNeLux countries in Europe. At the end of March 2013, a total of 110,521 meteoroid trajectories were measured that meet the selection criteria that the radiant position was more accurately than $\pm 2^\circ$ (1σ) and the apparent entry speed better determined than 10%. Typical precisions were 0.22° and 0.89% (0.37 km/s), respectively. This dataset was analyzed to extract meteor showers. In the mean time, the total of observed meteoroid trajectories by the California CAMS network has increased to $\sim 230,000$ as of March 31, 2015.

In an earlier paper (Jenniskens et al., 2016), we discussed how the established showers manifest in the 110,000 meteoroid orbits collected during the first 2.5 years of operations and how this data can be used in planetary science, satellite impact hazard mitigation, and planetary defense studies. In this paper, we will discuss a set of hitherto unconfirmed Working List showers that are now confirmed.

2. Methods

The CAMS project consists of a network of low-light Watec Wat902 H2 Ultimate video security cameras with 12-mm f1.2 Pentax lenses, each with a 20° by 30° field of view (Jenniskens et al., 2011). Meteors as faint as +5.4 magnitude are detected and the video is recorded in NTSC-format (640 by 480 pixel) interlaced frames at 60 fields/s. Data is stored in a 4-frame compression format that does not degrade the astrometric precision of the 8-s averaged frames, which contain background stars to +8.1 magnitude. Together, 20 cameras at a given station monitor the sky above 30° elevation. Stations are located at Fremont Peak Observatory, at Lick Observatory, and in Sunnyvale in California ($+37^\circ\text{N}$, 122°W). In addition to these 60 cameras, a handful of single cameras are operated by local amateur astronomers. A second, smaller but growing, network of cameras is distributed in the BeNeLux countries ($+51^\circ\text{N}$, 5°E). Each meteor's position is derived from the known star background and the astrometric tracks of all stations are combined to triangulate the meteors that are seen from at least two stations, using a new method to optimize the trajectory fit and entry speed (Gural, 2012). From this, the pre-atmospheric orbital elements are calculated (Jenniskens et al., 2011). At the end of March 2013, 109,548 meteoroid orbits were measured by the California network. The CAMS BeNeLux network added another 973.

To confirm previously reported meteoroid streams, the CAMS meteoroid orbit database was examined using an interactive software tool *CAMS StreamFinder*, which was developed to display the drift-corrected radiant and orbital elements, and equipped with algorithms to interactively isolate groups of meteoroid orbits from the data. For the specified range of solar longitude or date, the tool plots the radiant positions of all meteoroids (the Sun-centered geocentric declination versus right ascension), as well as the inclination (i) versus longitude of perihelion (II) of each meteoroid orbit. All known showers in the Working List are marked.

In this work, only those streams are confirmed that have a surface density significantly above that of the nearby sporadic meteor background in maps of meteoroid radiants (the direction from which the meteoroid approaches Earth) after removing the radiant drift caused by Earth's motion around the Sun. That radiant drift is calculated by adopting that the ecliptic radiant coordinates

of Longitude and Latitude (λ, β) are drifting by $\Delta\lambda = 1^\circ$ per degree of solar longitude λ_\odot interval and $\Delta\beta = 0^\circ$ per interval, respectively, and the result is then re-projected into the more familiar equatorial coordinate system of Right Ascension (R.A.) and Declination (Dec.).

To derive the median orbital elements of each shower (Jopek et al., 2006), meteoroids are isolated based on their similarity to a starting orbit. As a starting orbit, we used the radiant and speed or orbital elements reported in the IAU Working List. Observed meteoroid orbits are then compared to this orbit by means of a discriminant criterion (D). For a given threshold value, the analyst compares the selected meteors to the overall distribution of radiants and orbital elements nearby and adjusts the threshold D -value to isolate just enough similar meteoroid orbits from the background to remove the excess number density from the sporadic background. When adjusting the threshold value, the program identifies the meteors that are similar and plots those in a different color. "Just enough" in this context means that the distribution of extracted orbits does not significantly extend beyond the visually identified cluster. This is a conservative approach to identifying what meteoroids belong to a stream. Goal here is not to isolate all orbits that could potentially have originated from the same parent body, but to isolate those orbits that most probably originated from the same parent body.

We implemented a number of D -criteria based on orbital elements, specifically the Southworth and Hawkins (1963) D (without angular elements) and D_{sh} (with angular elements), the modified Southworth & Hawkins criteria D_{h} by Jopek (1993) and D_{v} by Jopek et al. (2008), the Drummond criterion D_{d} (Drummond, 1981), and the D_{b} criterion (Jenniskens et al., 2009). In addition, the D_{h} criterion (Valsecchi et al., 1999) and D_{rad} criterion (Holman and Jenniskens, 2013) are available to the user of CAMS Streamfinder, which isolate meteors based on the radiant position and entry speed. We found that the D_{h} criterion proved to be effective in isolating nearly all clusters in our application.

The radiant in ecliptic coordinates is drift-corrected to an integer solar longitude value. The drift-corrected ecliptic coordinates are then translated to equatorial coordinates. Typically, the integer solar longitude value was chosen nearest to the median solar longitude of the observed stream. However, because of data gaps, the peak of the shower is not always the median solar longitude of the extracted shower members. In some cases, we chose to drift-correct to the previously reported shower peak, in order to directly compare our measured radiant position to that of previously reported values. Because this baseline solar longitude is only used to drift-correct the radiant positions, this value can be adjusted after the stream has been extracted, recalculating the corresponding radiant position. By also providing the radiant drift rate, the tabulated radiant position can easily be adjusted once more information becomes available on when exactly is the peak of the shower.

3. Results

The confirmed showers will now be presented in order of their IAU number. Tables 1–3 present the median values of the radiant position and speed, as well as that of their orbital elements. Table 4 presents the dispersion of the radiant and speed, as well as the standard error in the median values.

Jenniskens et al. (2011) defines how the orbital elements from the pre-atmospheric (osculating) orbit of an individual meteoroid are derived. The values for each orbital element presented in Table 1 are the median value of the distribution of individual orbits, where the semi-major axis (a) is the inverse of the median value of $1/a$. T_j is the median Tisserand parameter with respect to

Table 1

Shower radiant and orbit, for showers listed in Jenniskens (2006) – N is number of extracted meteoroids; λ_o = chosen solar longitude to which radiant drift was corrected; R.A., Dec., V_g = equatorial coordinates and speed of the drift-corrected geocentric radiant (median values); orbital elements, median value of distribution: a = semi-major axis, derived from median value of $1/a$; q = perihelion distance; e = eccentricity, i = inclination, ω = argument of perihelion; Node = Node, Π = longitude of perihelion; T_j is the median Tisserand parameter with respect to Jupiter calculated from median values of orbital elements. Potential parent bodies are identified.

IAU	Object	N	λ_o	R.A.	Dec.	V_g	a	q	e	i	ω	Node	Π	T_j
21	AVB	12	32	203.5	+2.9	18.8	2.55	0.744	0.716	7.0	247.9	30.0	278.3	3.01
	?1998 SH2	<i>H</i>	28.9	195.9	−1.9	18.0	2.70	0.760	0.719	2.4	245.3	28.9	274.2	2.93
45	PDF	16	7	269.5	+65.9	23.4	2.66	0.996	0.626	38.4	178.1	7.2	187.1	2.83
	?2008 GV	<i>P</i>	15.7	265.6	+72.2	18.4	2.03	1.000	0.507	30.1	177.3	15.7	193.0	2.91
69	SSG	70	86	273.2	−29.5	25.1	2.02	0.457	0.769	6.0	104.5	266.4	10.8	3.37
88	ODR	63	110	259.3	+55.8	19.6	2.78	1.013	0.637	30.3	188.2	104.4	292.8	2.85
	?2013 LE16	<i>H</i>	86.2	258.3	+57.0	20.5	2.56	1.006	0.608	32.7	192.9	86.2	279.1	2.97
179	SCA	20	118	319.5	−10.9	34.1	2.10	0.192	0.911	8.4	314.8	111.8	66.3	3.00
	?2003 MT9	<i>P</i>	121.6	321.7	−10.2	34.5	2.54	0.200	0.921	8.7	312.4	121.6	74.0	2.59
186	EUM	45	89	233.3	+53.9	15.2	2.63	1.015	0.617	22.1	185.5	89.4	275.1	3.01
220	NDR	51	172	267.7	+54.0	18.9	2.90	1.004	0.654	28.8	182.0	171.7	349.5	2.78
	?2010 QA5	<i>P</i>	174.1	260.7	+61.1	21.1	2.73	1.004	0.633	33.5	176.2	174.1	350.3	2.75
253	CMI	32	252	102.4	+14.5	40.2	1.88	0.074	0.961	29.2	152.5	72.2	225.8	3.00

Symbol "?" indicates an uncertain parent body association.

Table 2

Newly confirmed CMOR showers. Parameters are defined as in Table 1.

IAU	Object	N	λ_o	R.A.	Dec.	V_g	a	q	e	i	ω	Node	Π	T_j
347	BPG	11	42	354.3	+30.8	44.2	5.16	0.347	0.944	69.1	68.0	42.3	108.5	1.24
362	JMC	32	77	15.8	+55.4	41.7	6.04	0.629	0.913	68.5	100.6	77.4	175.1	1.09
386	OBC	28	205	45.8	+52.3	43.6	5.69	0.387	0.932	68.6	286.3	205.2	130.9	1.19
394	ACA	30	245	98.6	−17.1	43.3	4.28	0.505	0.909	68.3	91.3	64.7	159.5	1.36
398	DCM	7	272	117.3	−12.5	42.9	4.21	0.388	0.916	60.3	105.6	91.0	197.4	1.55

Table 3

Newly confirmed video-detected meteor showers. Parameters are defined as in Table 2.

IAU	Object	N	λ_o	R.A.	Dec.	V_g	a	q	e	i	ω	Node	Π	T_j
340	TPY	11	264	151.4	−24.4	63.2	16.5	0.929	0.968	121.1	27.5	83.8	112.5	−0.44
343	HVI	11	38	204.8	−11.5	17.2	2.28	0.742	0.659	0.9	72.7	218.2	290.9	+3.28
345	FHE	19	344	270.9	+41.5	42.8	5.66	0.971	0.932	71.3	163.6	343.9	147.8	+0.75
410	DPI	13	92	11.2	+5.6	69.0	7.96	0.915	0.905	178.3	144.3	92.3	233.7	−0.60
413	MUL	27	120	267.0	+41.9	18.1	2.88	0.981	0.659	26.5	204.0	120.8	323.9	+2.81
416	SIC	17	167	30.3	+63.9	52.3	8.84	0.890	0.909	95.3	220.1	167.8	27.6	+0.42
428	DSV	22	262	200.8	+5.8	66.2	8.18	0.565	0.971	151.5	97.9	261.8	6.4	−0.56
429	ACB	11	308	231.7	+27.7	57.0	16.9	0.984	0.943	104.1	176.3	307.8	124.2	+0.01
431	JIP	11	94	332.1	+29.1	58.5	7.44	0.903	0.928	112.8	219.9	94.1	313.9	−0.02
458	JEC	11	83	316.1	+33.7	53.0	11.6	0.923	0.923	96.4	215.6	83.4	299.0	+0.30
480	TCA	11	206	137.1	+29.4	67.2	4.88	0.816	0.835	156.9	126.9	205.6	330.3	+0.09
510	JRC	14	84	320.5	+44.1	50.9	1.40	1.006	0.996	89.3	191.0	84.5	275.3	+0.04
512	RPU	22	231	130.4	−26.3	57.8	9.40	0.987	0.915	107.0	349.4	50.8	50.2	+0.09
519	BAQ	27	46	322.6	−0.9	69.0	6.89	0.941	0.951	156.6	150.1	46.1	197.4	−0.82
520	MBG	18	58	304.0	−15.6	65.8	9.39	0.546	0.959	170.9	265.5	58.7	325.7	−0.48
523	AGC	15	156	354.2	+76.6	43.9	11.4	1.005	0.913	75.6	188.1	156.1	344.7	+0.73
524	LUM	4	214	157.8	+50.2	60.9	3.10	0.920	1.008	114.5	148.5	213.5	4.1	−0.53
526	SLD	13	221	162.0	+68.2	49.1	4.47	0.987	0.779	89.0	188.5	221.1	50.3	+1.19
529	EHY	84	257	132.3	+2.5	62.4	9.98	0.362	0.981	142.2	106.1	78.4	184.7	−0.31
530	ECV	16	302	192.1	−18.1	68.1	5.29	0.823	0.847	158.4	49.8	122.2	171.1	−0.01
531	GAQ	26	58	314.0	+16.8	62.5	7.29	0.998	0.906	124.0	193.6	58.3	250.0	−0.19
533	JXA	20	119	41.5	+10.7	68.9	10.7	0.860	0.952	170.4	312.4	292.7	244.2	−0.81
	?C/1964 N1	<i>H</i>	107	31.5	+8.3	69.0	53.5	0.822	0.985	172.3	307.8	286.9	234.7	−1.01
549	FAN	76	112	20.5	+46.6	60.2	7.29	0.898	0.922	117.9	139.8	118.0	261.4	−0.09
555	OCF	14	189	48.8	+67.4	50.9	7.74	0.804	0.942	89.5	234.4	188.7	63.0	+0.39
563	DOU	5	269	159.1	+43.3	56.1	9.49	0.527	0.958	106.0	264.8	268.0	173.5	+0.18
567	XHY	8	284	172.2	−28.9	64.7	15.1	0.940	0.954	129.1	24.7	104.4	128.5	−0.48
569	OHY	12	312	179.2	−34.9	58.2	6.20	0.673	0.891	114.0	70.9	133.3	205.1	+0.44
570	FBH	12	314	249.4	+24.3	55.3	8.44	0.899	0.932	98.8	145.3	314.2	101.9	+0.22

Symbol "?" indicates an uncertain parent body association.

Jupiter. Because it is strongly dependent on semi-major axis, T_j was calculated from the derived median values of orbital elements.

The reliability of each extraction was evaluated by calculating the number of assigned stream members inside the 2σ contour of the distribution over that in the nearby background (both unassigned and previously assigned meteors), averaged over a four-times bigger area. This defines a shower-to-background surface

density ratio (S/B) listed in Table 4. S/B = 1 means that the shower raises the local surface density a factor of two above the sporadic background. Typically, $S/B \leq 2$ would constitute tentative detections, while values larger than 3 are strong detections.

Because the sporadic background varies from one direction to the next, and strong nearby streams may interfere, the tabulated values do not fully express how well the stream is isolated from

Table 4
Shower dispersion – Data on shower duration in solar longitude (λ_o , °), the drift corrected radiant (RA and Dec.) and geocentric speed (V_g) measurement accuracy (\pm refers to the standard error, in ° or km/s) and dispersion (σ refers to one standard deviation, in ° or km/s), the drift rate of the apparent radiant ($\Delta/\Delta\lambda_o$), and the shower-to-background surface density ratio (S/B).

IAU #	λ_o Begin	λ_o Peak	λ_o End	$\Delta RA \pm$	$\Delta RA \sigma$	$\Delta Dec \pm$	$\Delta Dec \sigma$	$\Delta V_g \pm$	$\Delta V_g \sigma$	$\Delta RA/\Delta\lambda_o$	$\Delta Dec/\Delta\lambda_o$	S/B
21	25	32	37	0.4	1.4	0.6	2.1	0.2	0.8	+0.91	−0.36	6
45	358	7	16	2.3	9.3	0.8	3.3	0.4	1.5	+0.03	+0.00	4
69	77	86	104	0.4	3.0	0.2	1.5	0.2	1.6	+1.14	+0.03	5
88	90	110	115	1.1	8.4	0.6	4.9	0.2	1.9	+0.34	−0.07	2
179	102	118	122	0.5	2.4	0.4	1.7	0.6	2.7	+0.97	+0.31	2
186	78	89	95	1.0	7.0	0.9	6.0	0.1	0.9	+0.48	−0.24	2
220	156	172	180	1.5	10.4	0.7	5.1	0.2	1.8	+0.37	−0.02	2
253	243	252	265	0.7	3.8	0.3	1.7	0.6	3.6	+1.02	−0.09	4
347	36	42	48	0.9	3.1	0.8	2.5	0.7	2.4	+0.90	+0.40	3
362	58	77	84	1.0	5.6	0.4	2.3	0.4	2.4	+1.08	+0.38	29
386	194	205	216	0.7	3.9	0.4	2.0	0.4	1.9	+1.29	+0.27	3
394	239	245	257	0.6	3.4	0.6	3.0	0.4	2.2	+0.80	−0.06	4
398	268	272	273	0.9	2.5	0.4	1.1	0.7	1.7	+0.84	−0.19	2
340	251	264	267	0.2	0.8	0.3	1.0	0.2	0.8	+0.83	−0.35	5
343	38	38	44	0.6	2.0	0.6	2.1	0.2	0.8	+0.95	−0.36	10
345	336	344	351	1.1	4.7	0.9	3.9	0.8	3.6	+0.57	+0.01	2
410	88	92	102	0.4	1.3	0.2	0.7	0.2	0.7	+0.93	+0.39	11
413	110	120	130	0.9	4.5	1.1	5.6	0.2	1.2	+0.56	−0.02	3
416	156	167	176	1.0	4.3	0.5	2.0	0.4	1.8	+1.34	+0.34	15
428	249	262	271	0.1	0.7	0.2	0.8	0.4	1.7	+0.90	−0.37	2
429	306	308	316	0.4	1.2	0.7	2.3	1.2	3.9	+0.75	−0.24	4
431	91	94	96	0.6	2.0	0.2	0.5	0.3	1.0	+0.81	+0.35	7
458	82	83	85	0.4	1.5	0.1	0.5	0.2	0.6	+0.73	+0.29	18
480	203	206	208	0.3	0.9	0.3	1.0	0.2	0.5	+1.07	−0.29	5
510	82	84	87	0.5	1.9	0.2	0.7	0.3	1.0	+0.67	+0.31	7
512	226	231	237	0.6	2.6	0.3	1.5	0.6	2.9	+0.77	−0.26	6
519	37	46	63	0.3	1.8	0.3	1.4	0.4	2.3	+0.92	+0.32	20
520	49	58	64	0.3	1.4	0.1	0.4	0.2	0.8	+1.01	+0.23	8
523	152	156	161	1.5	1.8	0.4	1.5	0.3	1.1	+0.76	+0.40	2
524	213	214	215	0.4	0.8	0.2	0.4	0.5	1.0	+1.09	−0.37	7
526	219	221	222	0.8	2.8	0.4	1.6	0.2	0.8	+1.21	−0.38	7
529	248	257	274	0.3	2.6	0.1	1.3	0.2	1.9	+0.93	−0.27	19
530	296	302	309	0.3	1.0	0.4	1.6	0.2	0.7	+0.95	−0.39	7
531	46	58	64	0.4	2.0	0.4	2.1	0.3	1.5	+0.83	+0.28	1
533	100	119	129	0.5	2.0	0.2	0.8	0.2	0.7	+0.97	+0.30	12
549	104	112	141	0.3	2.9	0.3	2.6	0.2	1.9	+1.07	+0.37	10
555	185	189	195	1.5	5.6	0.5	1.7	0.5	1.7	+1.65	+0.26	4
563	264	269	272	0.8	1.8	0.2	0.3	0.5	1.1	+1.05	−0.37	2
567	279	284	291	0.6	1.7	0.3	0.8	0.3	1.0	+0.89	−0.39	6
569	306	312	319	0.7	2.5	0.6	2.1	0.5	1.7	+0.92	−0.40	9
570	310	314	320	0.7	2.4	0.5	1.7	0.4	1.3	+0.75	−0.14	5

the nearby sporadic background, nor how the radiants are dispersed. For that reason, finding charts are provided for each confirmed shower (Figs. 1–13). These figures are drift-corrected to the central peak solar longitude listed in Table 4, unless otherwise specified in the figure caption. Table 4 provides the calculated drift rate at the position of the radiant.

3.1. The early Harvard photographic showers

In this work, we confirm showers numbered 21, 45, 69 and 88. CAMS earlier confirmed the η -Virginids (#11, EVI) and ε -Geminids (#23, EGE) (Jenniskens, 2012), the Northern δ -Aquiriids (#26, NDA) (Holman and Jenniskens, 2012a), and the ν -Cygnids (#409, NCY) (Jenniskens and Haberman, 2013). The latter are now more appropriately named after the earlier identified ζ -Cygnids (#40).

The α -Virginids (#21, AVB) are among a variety of previously identified Virginid showers in April and May (Jenniskens, 2006), nearly all of which do not stand out well from the antihelion source. One exception is a significant cluster centered on R.A. = 203.5° and Dec. = +2.9° at $\lambda_o = 32^\circ$ (Fig. 1A, Table 1). We identify this cluster as the previously identified α -Virginids. Southworth and Hawkins (1963) had the radiant nearby at R.A. = 194.8°, Dec. = +5.9° (centered on $\lambda_o = 21.7^\circ$), after drift correction to $\lambda_o = 32^\circ$.

Our measured entry speed is 2.2 km/s higher. The discrepancies in radiant and peak time do not appear to be significant, given that Lindblad (1971a,b) put the radiant at R.A. = 198.4°, Dec. = −6.4° (Lindblad, 1971a) and R.A. = 195.8°, Dec. = +0.6° (Lindblad, 1971b), centered on $\lambda_o = 28.9^\circ$ and 31.8° , respectively.

The ϕ -Draconids (#45, PDF) are identified in CAMS data as a diffuse concentration in the $II-i$ diagram (Fig. 1B). The shower was detected by Cook et al. (1972) from only a few photographic orbits, with similar streams detected by Sekanina (1973, 1976) from radar data. Period of activity, right ascension of the radiant and entry speed are in good agreement. However, the declination of the stream was given at Dec. = 68–72°, while we have a median Dec. = 66°. The radiant is just above the toroidal ring.

The Southern μ -Sagittariids (#69, SSG) form a concentration of radiants at the lower declination end of the antihelion source during $\lambda_o = 77-104^\circ$ (Fig. 1C). The shower was detected by Lindblad (1971b) and Cook et al. (1972) from six photographed orbits. Radiant position and period of activity are in good agreement with CAMS data. Sekanina (1976) derived two very similar streams from radar data, one peaking around $\lambda_o = 91^\circ$, the other around $\lambda_o = 100^\circ$. Various authors extracted short-period orbits with semi-major axis $a = 1.9-2.9$ AU, inclination $i = 1.0-5.0^\circ$, and longitude of perihelion $II = -2.3-28.6^\circ$ (Jenniskens, 2006). The group isolated here has

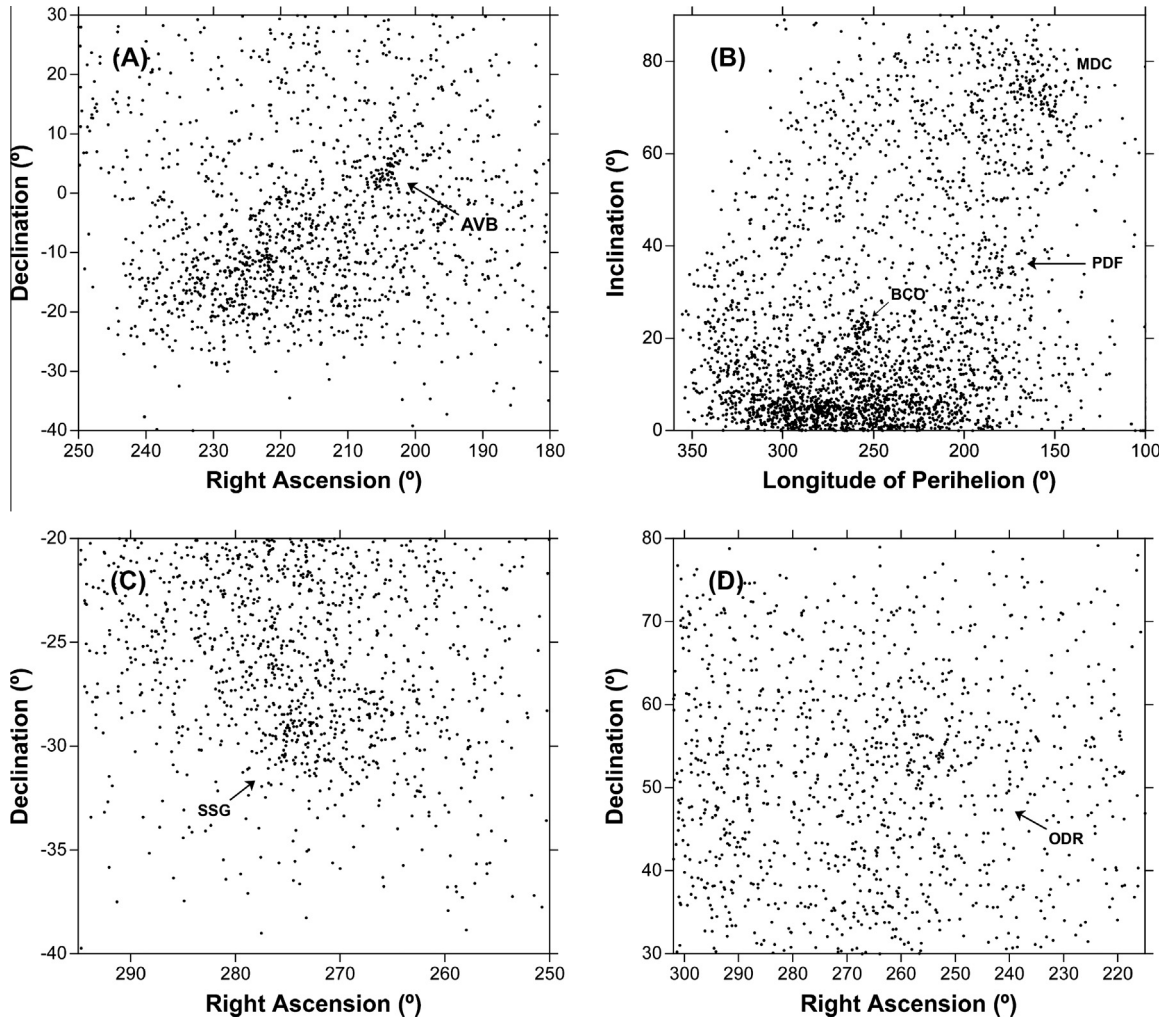


Fig. 1. (A) α -Virginids (#21, AVB) – period $\lambda_o = 25\text{--}37^\circ$; (B) ϕ -Draconids (#45, PDF) – period $\lambda_o = 358\text{--}16^\circ$; (C) Southern μ -Sagittariids (#69, SSG) – period $\lambda_o = 77\text{--}104^\circ$; (D) o-Draconids (#88, ODR) – period $\lambda_o = 90\text{--}115^\circ$.

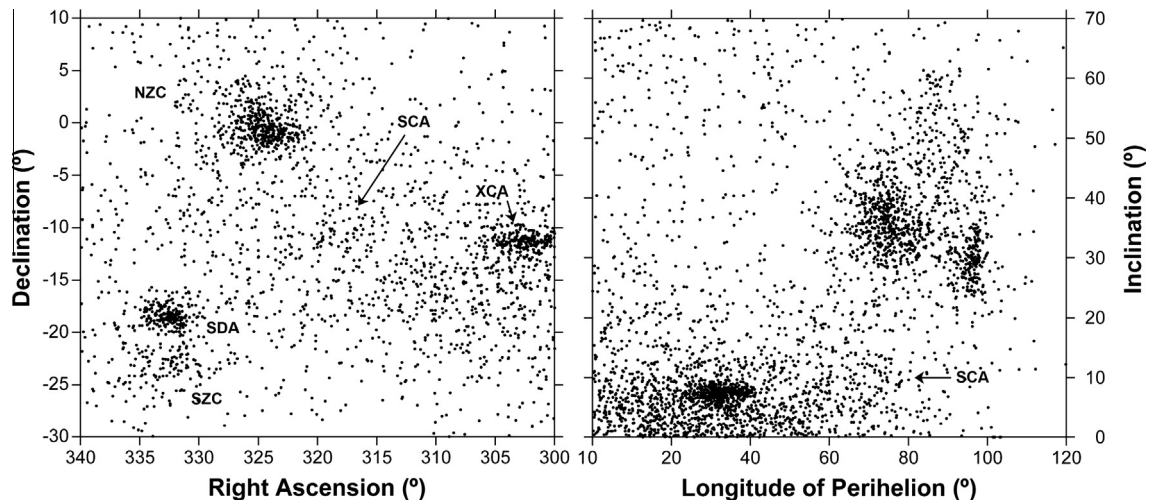


Fig. 2. σ -Capricornids (#179, SCA), – period $\lambda_o = 102\text{--}122^\circ$. Arrow points to a diffuse $\sim 5^\circ$ wide cluster.

median orbital elements $a = 2.02$ AU, $i = 6.0^\circ$, and $\Pi = 10.8^\circ$ (Table 1), suggesting that previous authors included some antihelion-source orbits with lower inclination in the sample.

Finally, the o-Draconids (#88, ODR) were identified by Cook et al. (1972) from three photographed orbits, which had a mean radiant at R.A. = 280° , Decl. = $+62^\circ$, and speed $V_g = 28.6$ km/s

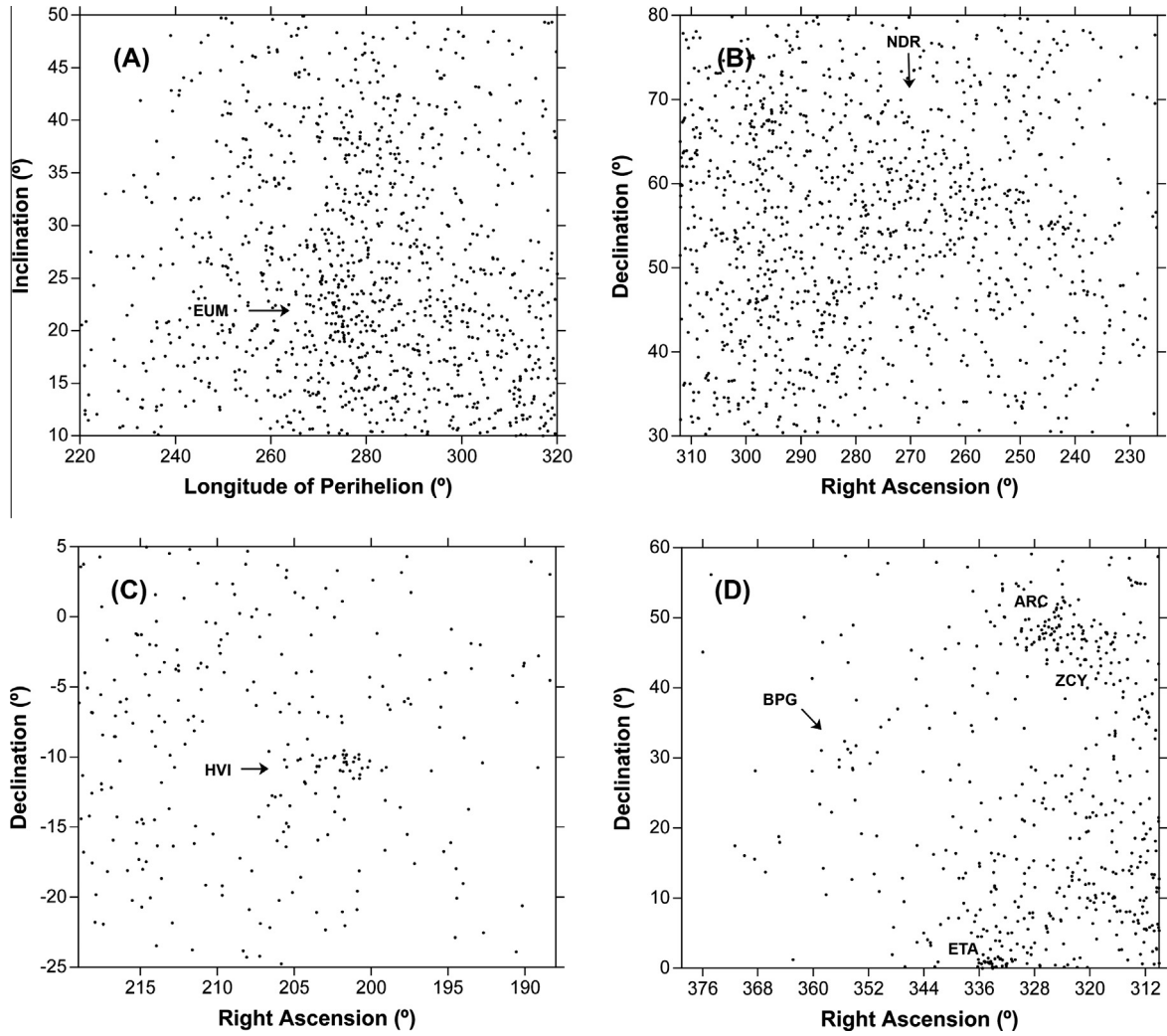


Fig. 3. (A) The ϵ -Ursae Majorids (#186, EUM) – period $\lambda_o = 78\text{--}95^\circ$; (B) ν -Draconids (#220, NDR) – period $\lambda_o = 156\text{--}180^\circ$; (C) η Virginids (#343, HVI) – period $\lambda_o = 38\text{--}44^\circ$; (D) β -Pegasids (#347, BPG) – period $\lambda_o = 36\text{--}48^\circ$.

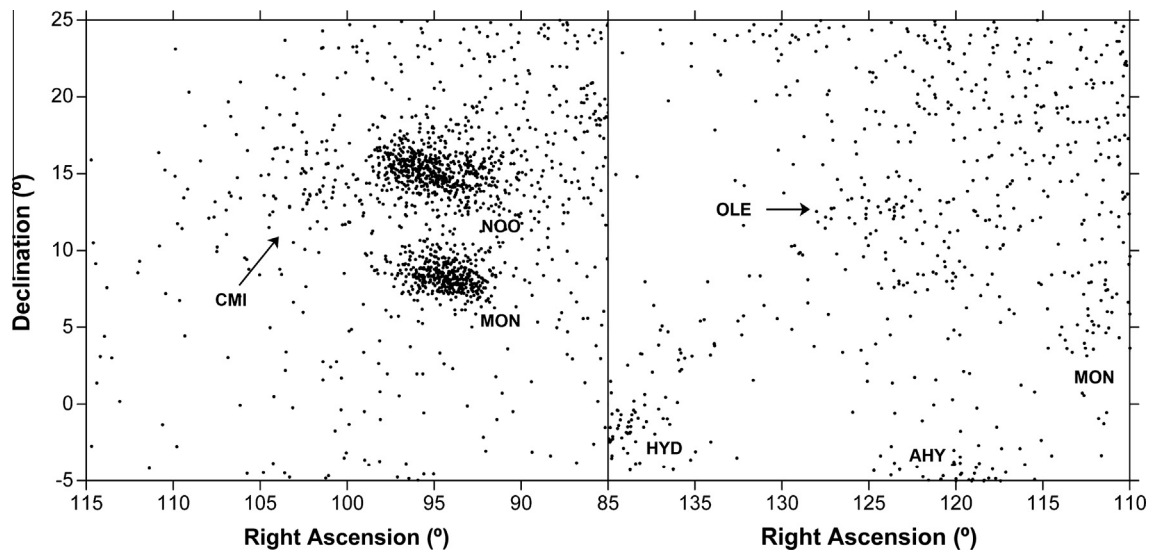


Fig. 4. Left: December Canis Minorids (#253, CMI) – period = $243\text{--}265^\circ$. Right: o-Leonids (#515, OLE) in period $\lambda_o = 269\text{--}283^\circ$, but likely same shower as CMI.

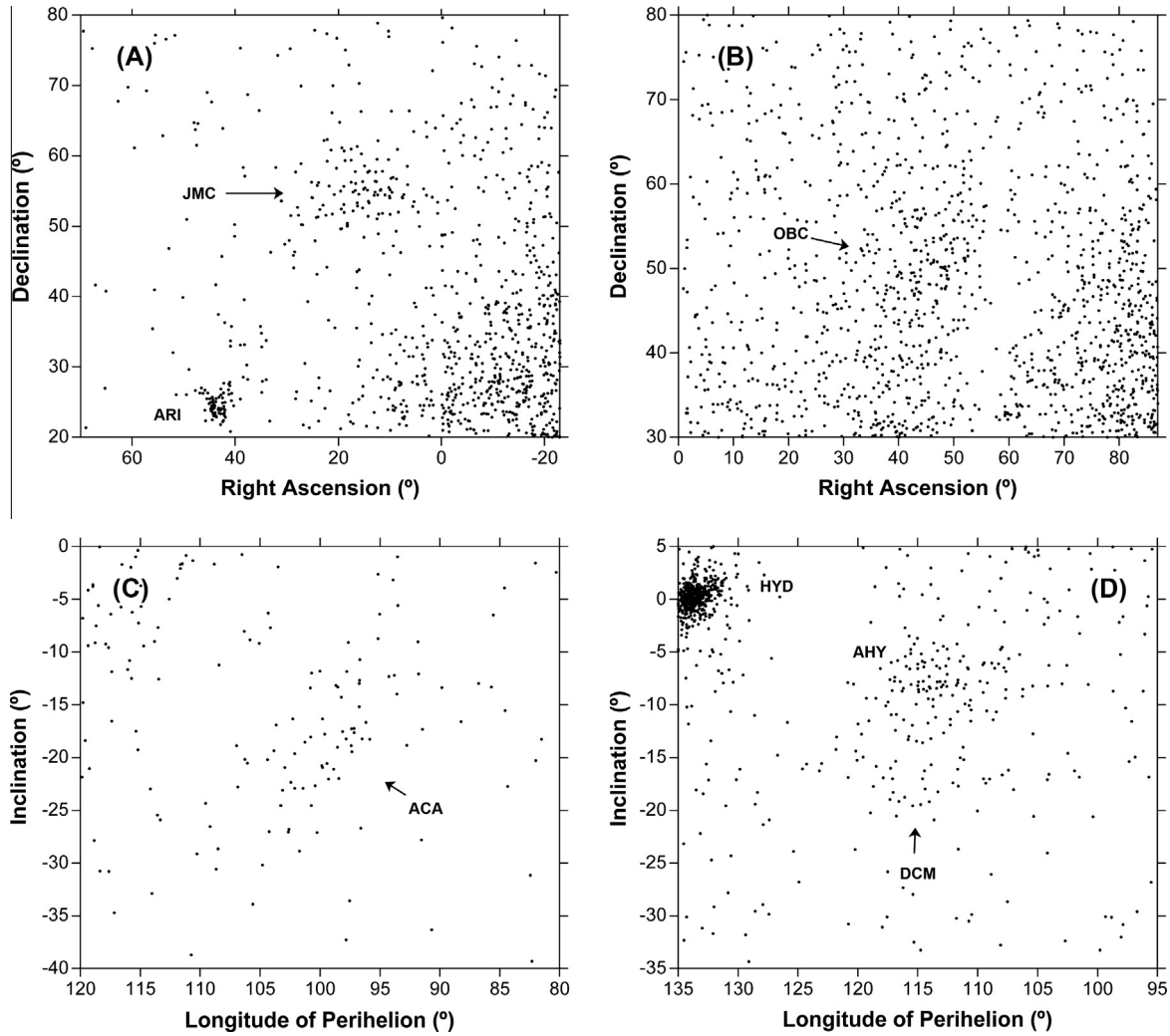


Fig. 5. (A) June μ -Cassiopeiids (#362, JMC) – period $\lambda_o = 58\text{--}84^\circ$; (B) October β -Camelopardalids (#386, OBC) – period $\lambda_o = 194\text{--}216^\circ$; (C) α -Canis Majorids (#394, ACA) – period $\lambda_o = 239\text{--}257^\circ$; (D) December Canis Majorids (#398, DCM) – period $\lambda_o = 257\text{--}273^\circ$ (drift corrected to 266°).

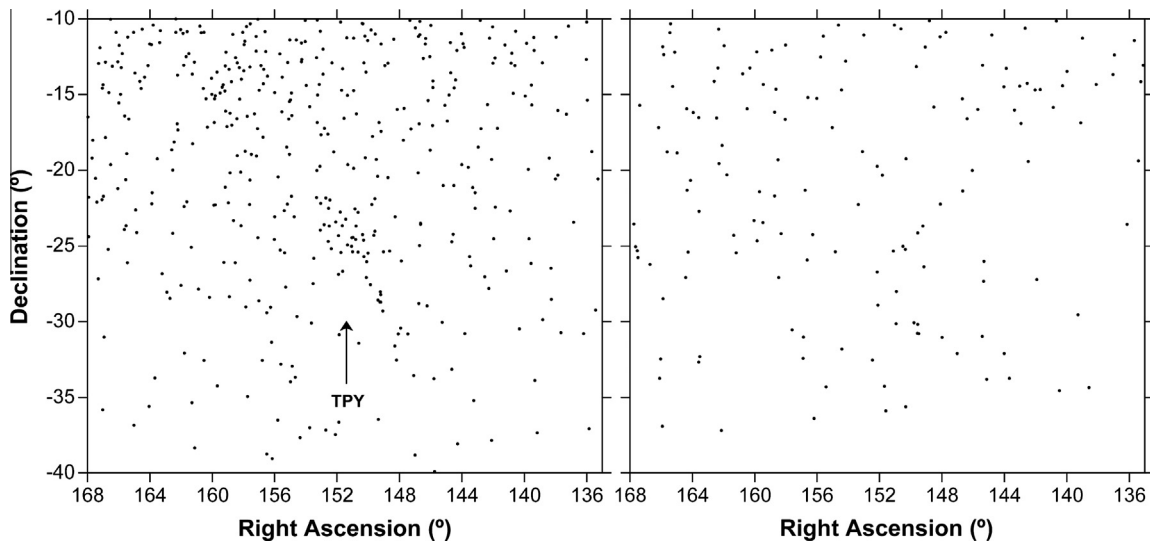


Fig. 6. 0-Pyxidids (#340, TPY) – Left: period $\lambda_o = 251\text{--}267^\circ$; Right: period $\lambda_o = 245\text{--}251^\circ$.

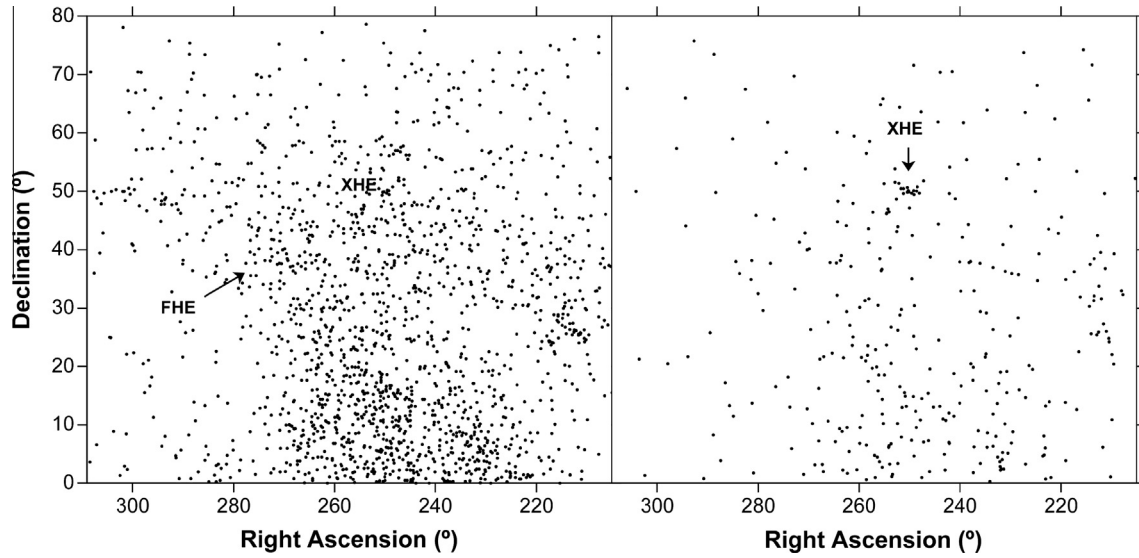


Fig. 7. Left: The diffuse f-Herculids (#345, FHE) – period $\lambda_0 = 336\text{--}352^\circ$. Right: the already established x-Herculids (#346, XHE) – period $\lambda_0 = 349\text{--}352^\circ$. Both graphs are drift corrected to 344° .

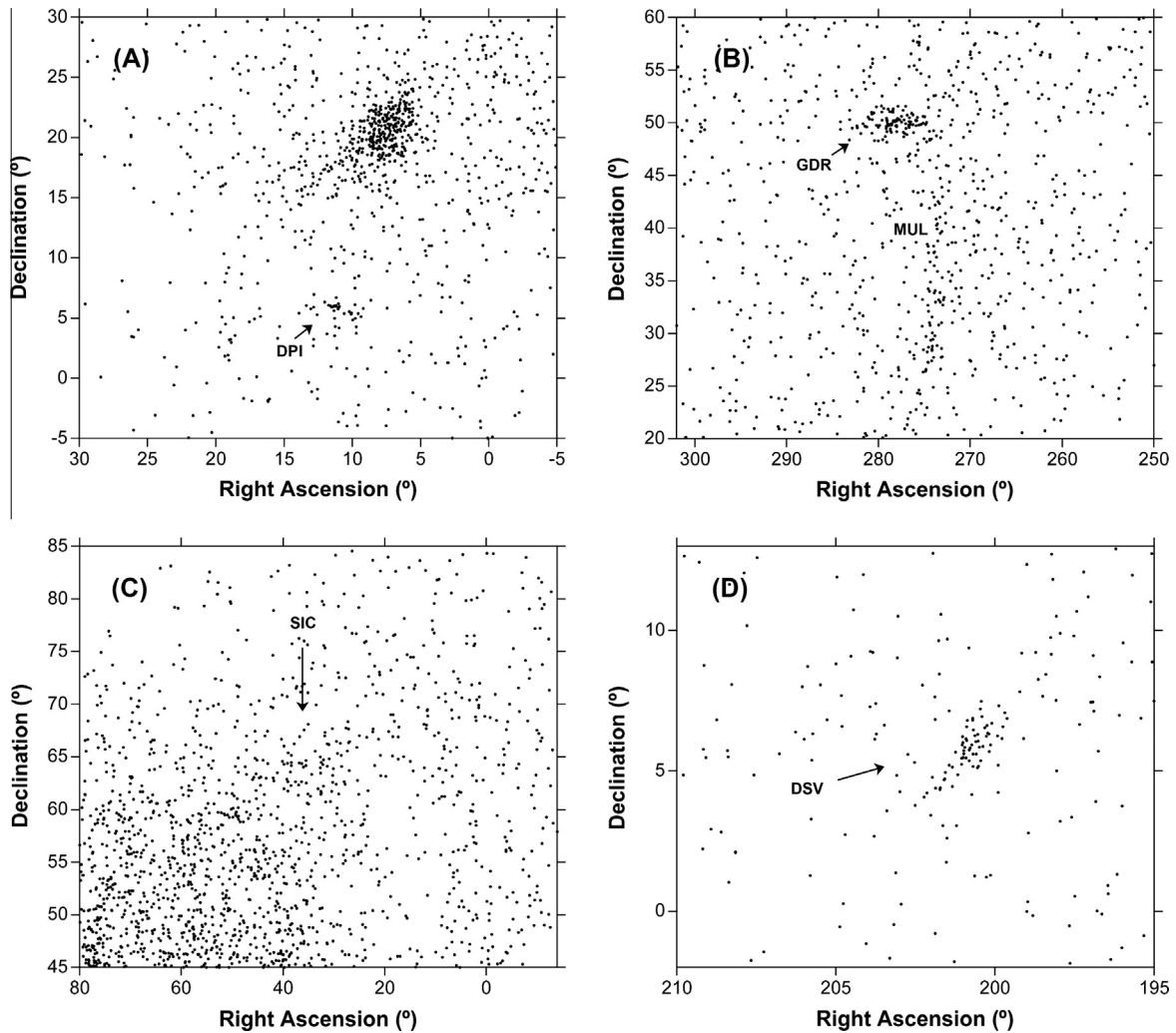


Fig. 8. (A) δ -Piscids (#410, DPI) – period $\lambda_0 = 88\text{--}102^\circ$; (B) μ -Lyrids (#413, MUL) – period $\lambda_0 = 120\text{--}130^\circ$; (C) September ι -Cassiopeiids (#416, SIC) – period $\lambda_0 = 156\text{--}176^\circ$; (D) December σ -Virginids (#428, DSV) – period $\lambda_0 = 249\text{--}271^\circ$.

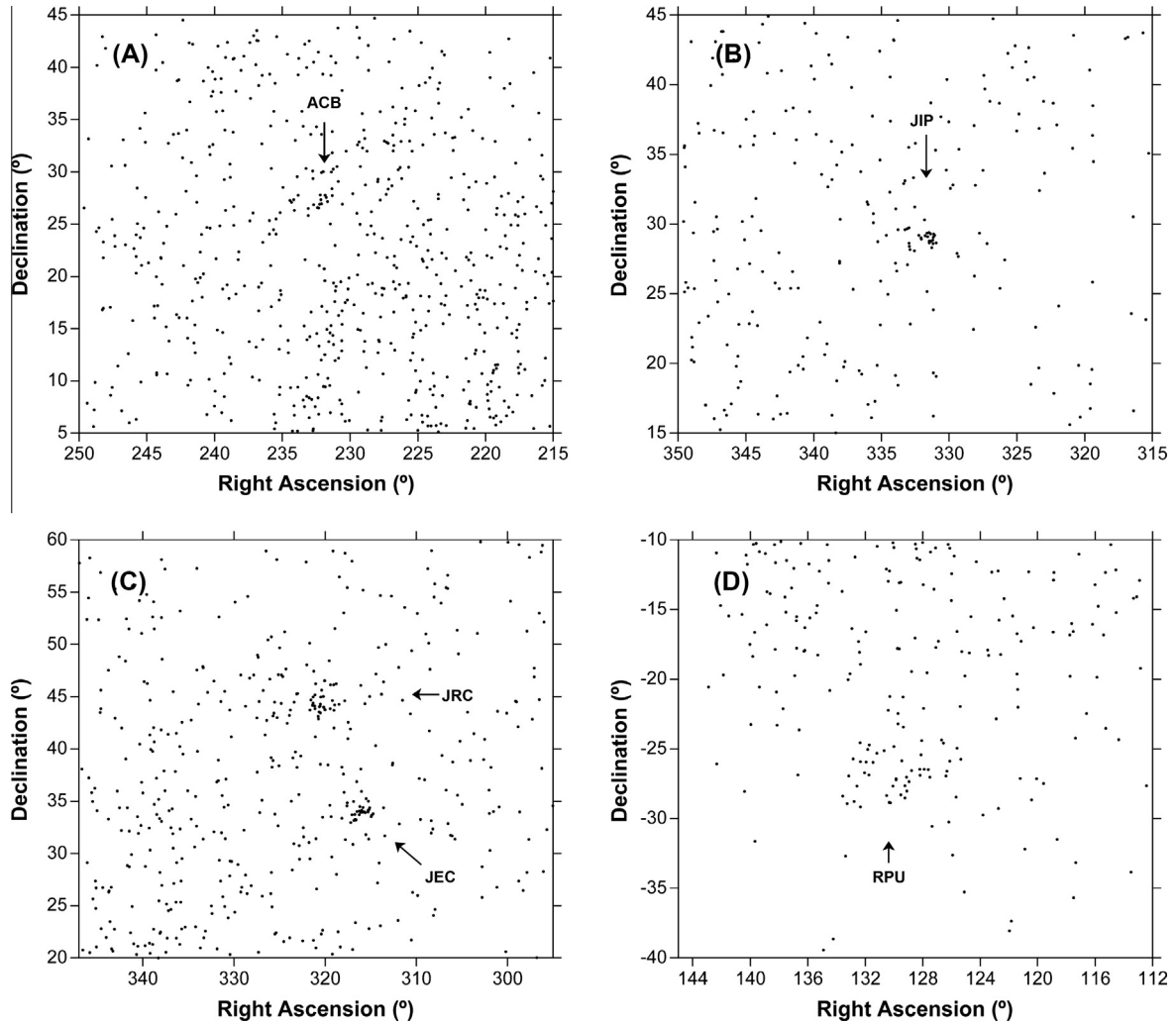


Fig. 9. (A) α -Coronae Borealis (#429, ACB) – period $\lambda_0 = 306\text{--}316^\circ$; (B) June ι -Pegasis (#431, JIP) – period $\lambda_0 = 91\text{--}96^\circ$; (C) June ρ -Cygnids (#510, JRC) and June ε -Cygnids (#458, JEC) – period $\lambda_0 = 82\text{--}87^\circ$ (drift corrected to 84°); (D) ρ -Puppids (#512, RPU) – period $\lambda_0 = 226\text{--}237^\circ$.

around $\lambda_0 = 114^\circ$. A similar stream was detected by radar (Sekanina, 1976). No stream was found at the reported position in CAMS data. However, we did have a nearby concentration of orbits at R.A. = 259° , Decl. = $+56^\circ$, with lower $V_g = 19.6$ km/s (Fig. 1D). Rather than assign a new name, we considered the position close enough to assign these meteors to the ODR. However, the lower entry speed translates to a significantly lower inclination $i \sim 30^\circ$ than reported before ($43\text{--}46^\circ$). The perihelion distance $q = 1.013$ AU is slightly higher than that reported earlier ($q = 1.006, 1.010$ AU). Also, we have $\Pi = 293^\circ$, compared to $\Pi = 304$ and 308° by Cook et al. (1972) and Sekanina (1976), respectively.

3.2. Showers from the Working List by Jenniskens (2006)

Table 1 lists results for four showers that are now confirmed from the Working List by Jenniskens (2006). CAMS earlier confirmed the Northern delta-Cancrids (#96, NCC) and Southern delta-Cancrids (#97, SCC) (Jenniskens et al., 2016), the Northern June Aquilids (NZC, IAU #164) (Holman and Jenniskens, 2012a), the July Pegasus (#175, JPE) (Holman and Jenniskens, 2013), the July γ -Draconids (#184, GDR) (Holman and Jenniskens, 2012b), as well as the August Draconids (#197, AUD) and the α -Lyncids (#252, ALY) (Jenniskens, 2012). Jenniskens et al. (2016) also assigned various Taurid shower components to a number of

previously reported showers, the most well isolated being the Southern χ -Orionids (#257, ORS) (Jenniskens, 2012). Other shower components still need confirmation.

The σ -Capricornids (#179, SCA) are known from radar observations by Nilsson (1964) and Sekanina (1973, 1976). They are considered the strongest video-detected southern hemisphere meteor shower in early July in single-station IMO Video Meteor Network data by Molau and Kerr (2014), who reported a radiant at R.A. = 313° , Dec. = -5° , for $V_g = 39$ km/s. Instead, we find a weak excess at R.A. = 320° , Dec. = -11° in between much more prominent showers (Fig. 2). These meteors have a slightly higher entry speed $V_g = 34$ km/s than the radar-observed meteors ($V_g = 25\text{--}30$ km/s), which is not uncommon. In the Π - i diagram, the shower stands out from other ecliptic meteoroids by having a higher inclination and longitude of perihelion (Fig. 2).

The ε -Ursae Majorids (#186, EUM) were identified from photographic orbits by Terentjeva (1989): a slow shower with R.A. = 193° , Dec. = $+62^\circ$, and $V_g = 15.2$ km/s, corresponding to $\Pi = 262^\circ$ and $i = 20^\circ$ (Jenniskens, 2006). We only see a weak enhancement in the radiant map, but find a nearby concentration in Π - i space at $\Pi = 275^\circ$ (Fig. 3A).

The ν -Draconids (#220, NDR) were detected from radar data by Sekanina (1976), who put the radiant at R.A. = 265° , Dec. = $+60^\circ$, and $V_g = 20$ km/s. This compares to our $\sim 15^\circ$ diameter group centered on R.A. = 268° , Dec. = $+54^\circ$ and $V_g = 19$ km/s, in

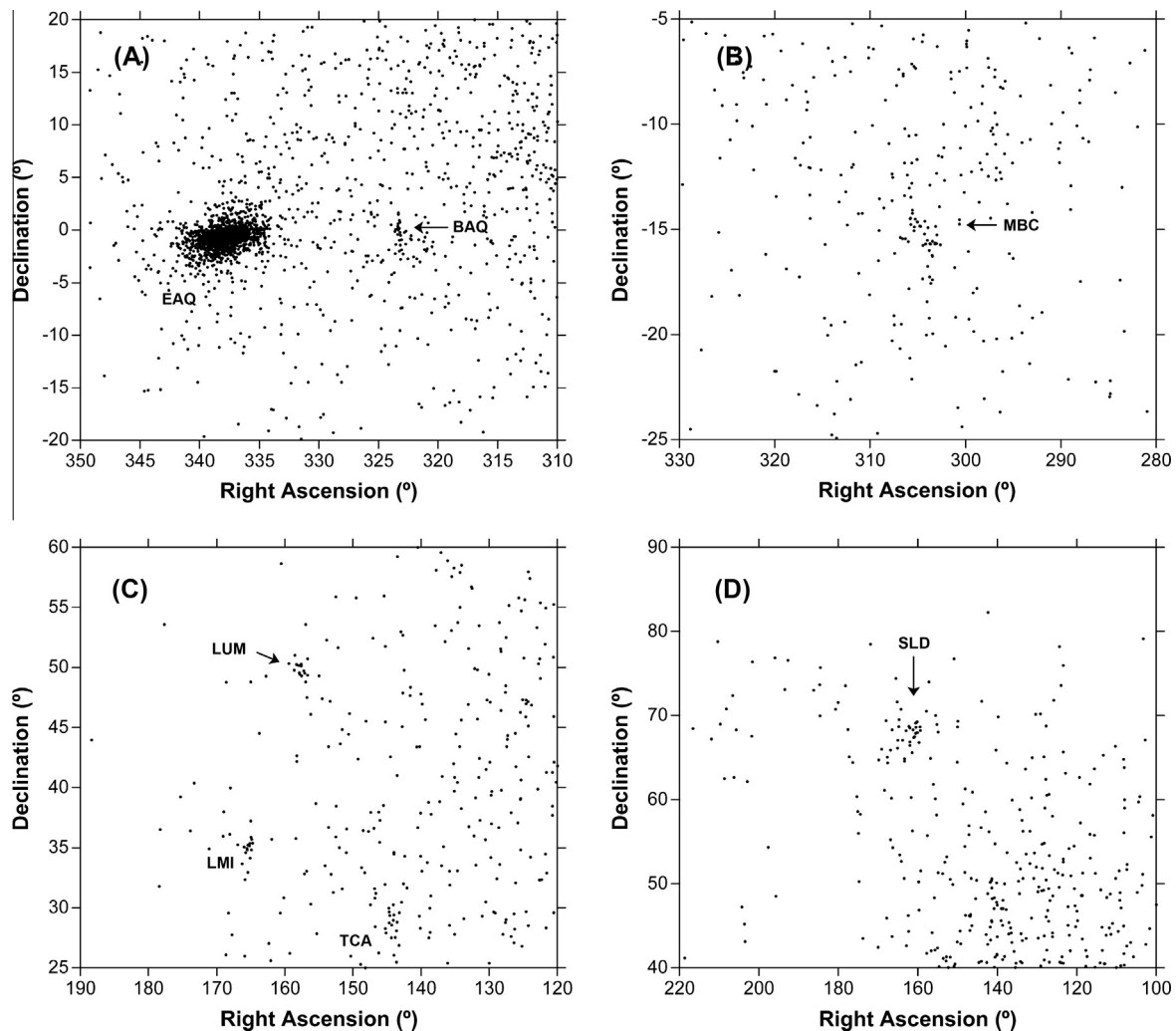


Fig. 10. (A) β -Aquariids (#519, BAQ) – period $\lambda_o = 37\text{--}63^\circ$; (B) May β -Capricornids (#520, MBC) – period $\lambda_o = 49\text{--}64^\circ$; (C) λ -Ursae Majorids (#524, LUM) – period $\lambda_o = 213\text{--}215^\circ$. Also shown are the established Leonis Minorids (#22, LMI) and the newly discovered τ -Cancriids (#480, TCA); (D) Southern λ -Draconids (#526, SLD) – period $\lambda_o = 219\text{--}222^\circ$.

good agreement. The group stands out from adjacent activity in both the radiant and $II-i$ diagrams only as a function of time (Fig. 3B).

The December Canis Minorids (#253, CMI) were identified by Jenniskens (2006) from only two photographed meteors and a visual report of a meteor outburst at $\lambda_o = 252.4^\circ$. CAMS detected meteors from this direction during the period $\lambda_o = 243\text{--}265^\circ$. In the following weeks, activity from the o-Leonids (#515, OLE) was detected (period $\lambda_o = 269\text{--}283^\circ$), which appears to be the same shower when corrected for radiant drift (Fig. 4).

3.3. The CMOR showers

Five more of the CMOR-discovered showers are confirmed (Table 2). CAMS earlier confirmed the April ρ -Cygnids (#348, ARC) (Phillips et al., 2011), the ϕ -Piscids (#372, PPS) (Holman and Jenniskens, 2013), as well as the χ -Taurids (#388, CTA), the o-Eridanids (#338, OER), and the November θ -Aurigids (#390, THA) (Jenniskens et al., 2011), the October Ursae Majorids (#333, OCU), the December α -Draconids (#334, DAD), the December χ -Virginids (#335, XVI), the December κ -Draconids (#336, DKD), the v-Eridanids (#337, NUE), the ϕ -Ursae Majorids (#339, PSU), the January χ -Ursae Majorids (#341, XUM), the x-Herculis (#346, XHE) (Jenniskens, 2012), the August Cetids (#379, ACT)

(Jenniskens, 2008), and the γ -Ursae Minorids (#404, GUM) (Jenniskens, 2012). The median orbital elements for these are tabulated in Jenniskens et al. (2016).

The β -Pegasisds (#347, BPG) are on the daytime side of the toroidal ring (Fig. 3D). The small group is well isolated in the $II-i$ diagram (not shown). In CAMS data, the shower peaks 6 days later ($\lambda_o = 36\text{--}48^\circ$). Our entry speed is 3.2 km/s higher than reported by Brown et al. (2010), resulting in a slightly higher inclination ($69.1 \pm 1.4^\circ$ rather than 62.7°) and wider semi-major axis ($a = 6.1 \pm 2.6$ AU, rather than ~ 2.76 AU).

The June μ -Cassiopeiids (#362, JMC) are also on the toroidal ring and are well detected, just above the established Daytime Arietids (#171, ARI) (Fig. 5A). CAMS data show a peak 3 days later, with a 1.9 km/s lower entry speed. The median semi-major axis of the shower is typical of other toroidal ring showers, rather than the higher value found for many apex-source showers.

The diffuse October β -Camelopardalids (#386, OBC) are detected during $\lambda_o = 194\text{--}216^\circ$, with a peak at 205° . Brown et al. (2010) put the peak at $\lambda_o = 214^\circ$ (Fig. 5B). Our speed of 43.6 km/s is less than that reported by CMOR: $V_g = 47.6$ km/s. Differences in radiant and speed, however, do not translate into significantly different orbital elements in this case.

The CAMS-detected α -Canis Majorids (#394, ACA) are on the southern part of the toroidal ring, close to the antihelion source

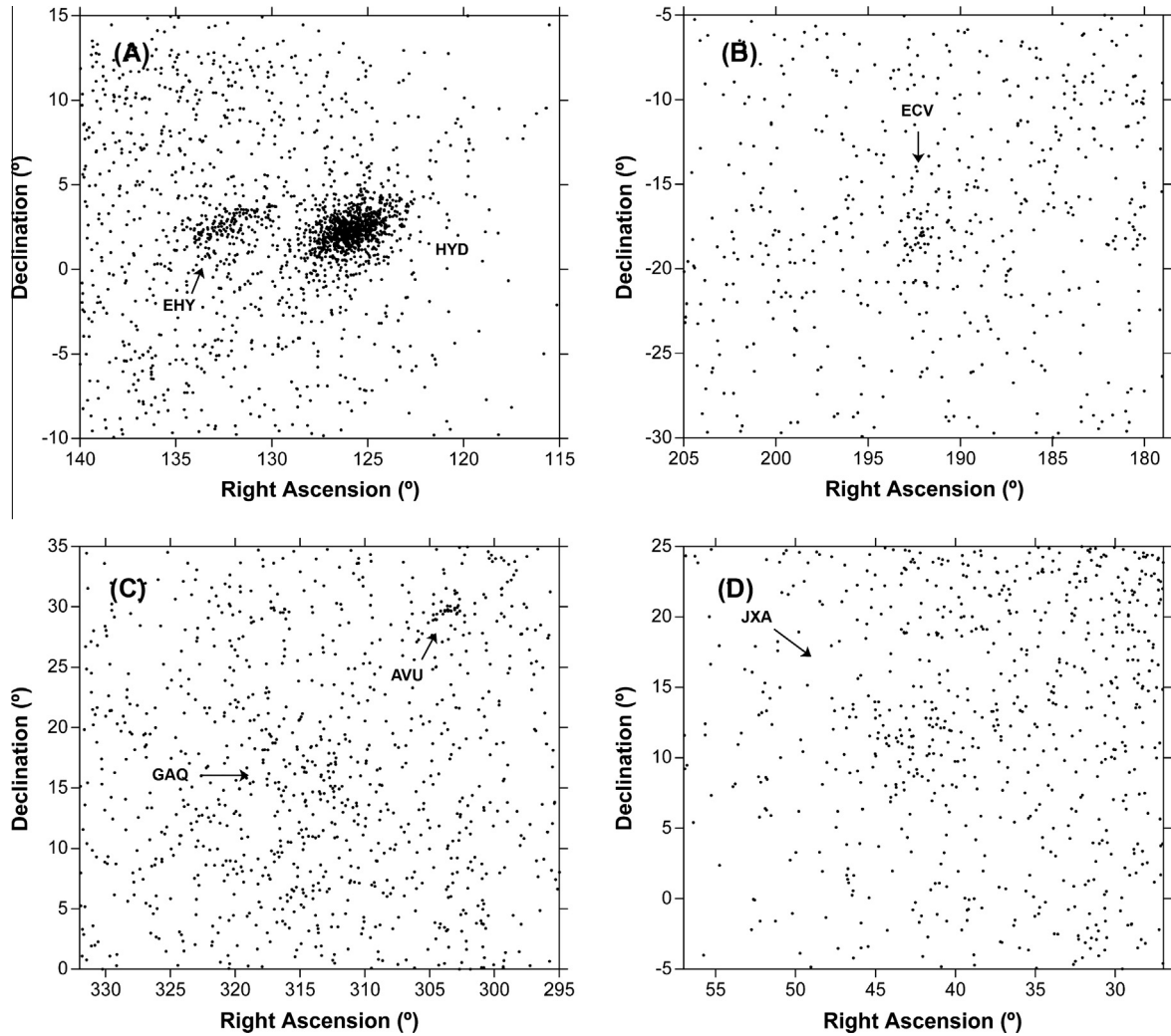


Fig. 11. (A) η -Hydrids (#529, EHY) – period $\lambda_o = 248\text{--}274^\circ$; (B) η -Corvids (#530, ECV) – period $\lambda_o = 296\text{--}309^\circ$; (C) γ -Aquilids (#531, GAQ) – period $\lambda_o = 46\text{--}64^\circ$. Also shown are the newly discovered α -Vulpeculids (#661, AVU); (D) July ξ -Arietids (#533, JXA) – period $\lambda_o = 100\text{--}129^\circ$.

(Fig. 5C). Radiant position and speed are in good agreement with Brown et al. (2010).

The December Canis Majorids (#398, DCM) are a weak diffuse shower just below the established α -Hydrids (#331, AHY) (Fig. 5D). They have a radiant and speed in good agreement with Brown et al. (2010). Few meteors were assigned to this stream in the initial extraction, with the group centered on $\lambda_o = 272^\circ$ rather than 266° .

3.4. The recently detected low-light video showers

Table 3 contains results for 28 newly confirmed showers previously detected in other video-based meteoroid orbit surveys. Finding charts are shown in Figs. 6–13. In previous papers, CAMS confirmed the c Andromedids (#411, CAN), the κ -Ursae Majorids (#445, KUM) (Jenniskens et al., 2012), and independently discovered outbursts of the February η -Draconids (#427, FED) (Jenniskens and Gural, 2011) and the December ϕ -Cassiopeiids (#445, DPC) (Jenniskens et al., 2012). An earlier paper also discussed the zeta Cassiopeiids (#444, ZCS) (Segon et al., 2012) and August iota Cetids (#505, AIC) as components of established stream complexes, as well as a number of less-well defined showers associated with the Orion tail (Jenniskens et al., 2016).

The θ -Pyxidids (#340, TPY) were identified from SonotaCo data by Kanamori (2009) and are now confirmed (Fig. 6). More recently, 28 meteors from SonotaCo and CMN data were assigned to this stream by Segon et al. (2014c) based on an automatic search routine. The shower is well defined. However, we find a peak 15 days later than reported before, with the period of activity ($251\text{--}267^\circ$) just outside the peak time of $\lambda_o = 249^\circ$ reported earlier. The shower is not detected in the interval $\lambda_o = 245\text{--}251^\circ$ (right diagram in Fig. 6).

The h Virginids (#343, HVI) was also identified from SonotaCo data by Kanamori (2009). More recently, 75 meteors were extracted from SonotaCo and CMN data by Segon et al. (2014c). CAMS has a strong detection (Fig. 3C). Peak time and radiant are in good agreement. The meteoroids move in a Jupiter-family comet type orbit.

The f-Herculids (#345, FHE) from Molau and Kac (2009) do correspond with a diffuse enhancement in surface density of meteoroid radiants (Fig. 7A). The contemporary x-Herculids (#346, XHE) are compact (Fig. 7B) and were earlier confirmed (Jenniskens, 2012).

The δ -Piscids (#410, DPI) are a compact shower in a low inclined retrograde orbit (Fig. 8A). Uncertainties in speed cause a wide range of argument of perihelion, for which none of the D-criterion extractions are effective. The stream was extracted by

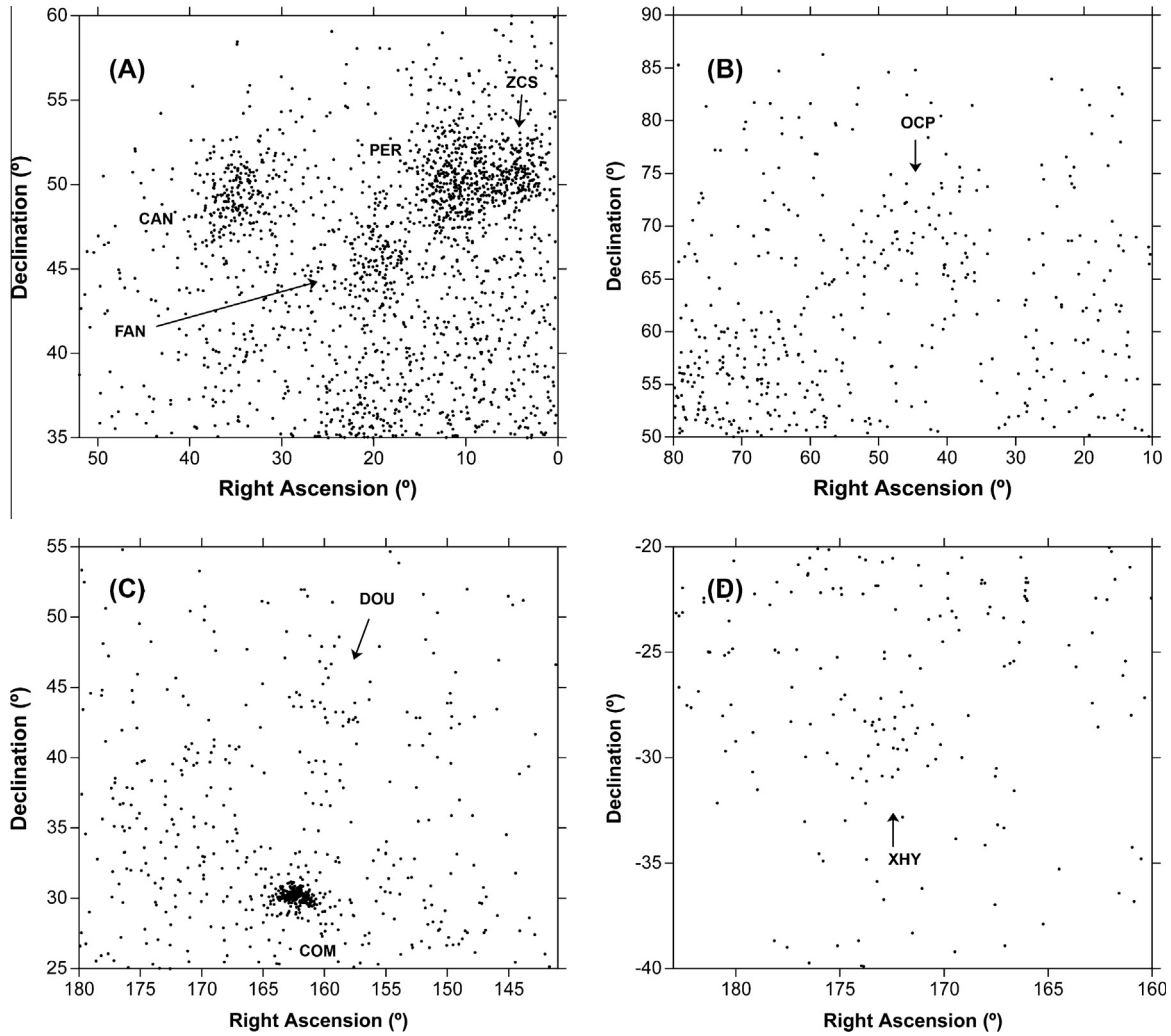


Fig. 12. (A) 49-Andromedids (#549, FAN) – period $\lambda_o = 104\text{--}125^\circ$ (drift corrected to 112°). Also shown are the Perseids (#7, PER), the ζ -Cassiopeiids (#444, ZCS), and the c Andromedids (#411, CAN); (B) October γ -Camelopardalids (#555, OCP) – period $\lambda_o = 185\text{--}195^\circ$; (C) December ω -Ursae Majorids (#563, DOU) – period $\lambda_o = 264\text{--}272^\circ$; (D) ξ -Hydrids (#567, XHY) – period $\lambda_o = 279\text{--}291^\circ$.

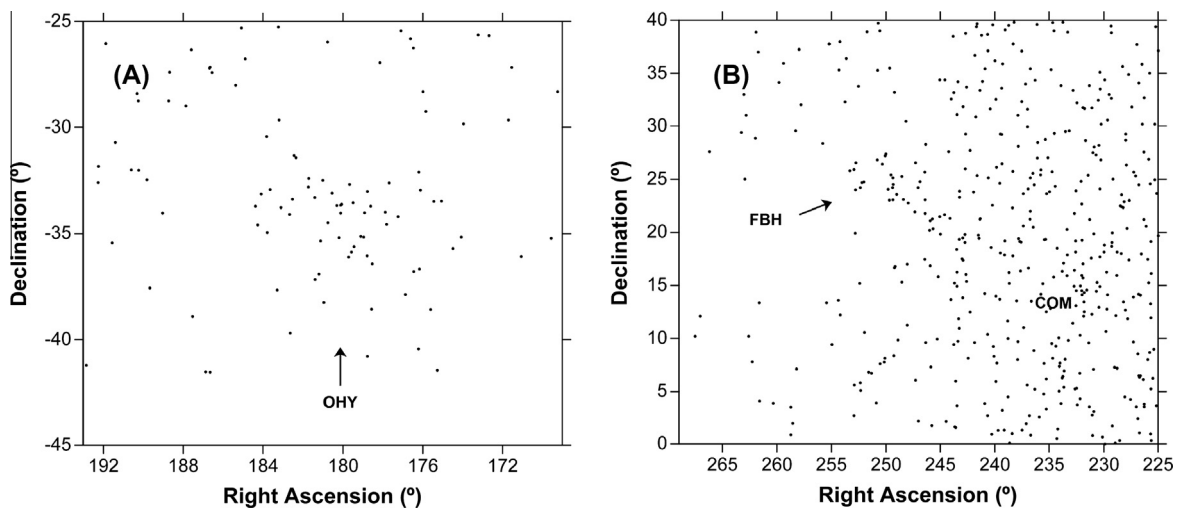


Fig. 13. (A) o-Hydrids (#569, OHY) – period $\lambda_o = 306\text{--}319^\circ$; (B) February β -Herculids (#570, FBH) – period $\lambda_o = 310\text{--}320^\circ$.

varying the starting orbit correspondingly. The shower has a peak time, radiant and entry speed in good agreement with Molau and Rendtel (2009), who discovered this shower in IMO Video Meteor Network data. Segon et al. (2014c) assigned 47 meteors to this stream.

The μ -Lyrids (#413, MUL) by Molau and Rendtel (2009) were reported to be at R.A. = 273°, Dec. = +39° at $\lambda_o = 116^\circ$. In recent CAMS data, that position is part of a band of radiants that stretches north in Declination toward the July gamma-Draconids (#184, GDR) during the period $\lambda_o = 110\text{--}130^\circ$ (Fig. 8B). This is reminiscent of a similar band seen in Andromedid shower radiants (Jenniskens et al., 2016). This band may well represent one shower, or shower component.

Molau and Rendtel (2009) also identified the September ι -Cassiopeiids (#416, SIC), which are shown in Fig. 8C. This is a diffuse high declination shower, a weak concentration in the toroidal source. Nevertheless, CAMS-derived data are in agreement with those reported from the IMO Video Meteor Network. Segon et al. (2014c) did not detect this shower.

The December σ -Virginids (#428, DSV) were identified from SonotaCo data by Greaves (2012). In more recent searches, Segon et al. (2014c) assigned 113 meteors. CAMS made a strong detection (Fig. 8D). They were hard to extract from the background, because the orbital elements appear to change during the solar longitude $\lambda_o = 245\text{--}275^\circ$ interval. Our maximum is 2° earlier than that reported by Greaves.

Greaves (2012) also identified the α -Coronae Borealids (#429, ACB) from SonotaCo data. Segon et al. (2014b) assigned 35 meteors. The shower is a narrow well-defined cluster in CAMS data (Fig. 9A) and was detected by CAMS in 2012 and 2015, with good agreement to previous reports.

Another of Greaves' (2012) showers, the June ι -Pegasids (#431, JIP), is compact and well defined (Fig. 9B). Segon et al. (2014b) assigned 16 meteors. The shower appeared annually in CAMS data from 2011 to 2014. All but three meteors were detected between $\lambda_o = 93.45$ and 94.28° . Greaves had a peak at $\lambda_o = 94.456^\circ$. Other results are in good agreement.

Showers #448–502 were identified by Rudawska and Jenniskens (2014) from combined SonotaCo and first year CAMS data. These are not strictly independent datasets from results presented here. Kornos et al. (2014) confirmed 18 of these showers, and made more tentative detections of another 12, based on automated searches in the independent EDMOND database. Some are very strong showers, detected in multiple years. One of these, the June ε -Cygnids (#458, JEC) is a strong compact shower in the current CAMS database. Most were detected between $\lambda_o = 81\text{--}84^\circ$ (Fig. 9C). Segon et al. (2014b) confirmed this shower from SonotaCo and CMN data, assigning 16 meteors. Another, the τ -Cancrids (#480, TCA) are shown in Fig. 10C. Perhaps not surprisingly, results for this shower are also in good agreement with what was reported before. Segon et al. (2014b) confirmed by assigning 52 meteors.

The June ρ -Cygnids (#510, JRC) are a similarly compact shower first identified by Segon et al. (2013a) from combined SonotaCo and Croatian Meteor Network data. CAMS results are in good agreement (Fig. 9C).

The ρ -Puppids (#512, RPU) were first identified by Segon et al. (2013a). This shower is now confirmed by CAMS (Fig. 9D). The drift-corrected radiant and speed are in good agreement. Segon et al. reported a peak at $\lambda_o = 223^\circ$, 8 days earlier than our peak at $\lambda_o = 231^\circ$ during an activity period 223–237°. In this case, a few possible shower meteors were detected in the days before $\lambda_o = 223^\circ$ in the more recent CAMS data, implying that the shower is active earlier than found from the March 2013 data alone.

CAMS detected the β -Aquiriids (#519, BAQ) much as reported by Andreic et al. (2013) (Fig. 10A). The measured orbits have a wide range of entry speed, resulting in a wide range of longitude of perihelion. The range in inclination is narrow, suggesting orbital evolution at work.

Andreic et al. (2013) also reported the May β -Capricornids (#520, MBC). CAMS results are in good agreement (Fig. 10B). Molau and Kerr (2014) detected single-station meteors radiating from this general direction.

Initially only detected as a tight cluster of four meteors, the more recent CAMS orbit catalogue shows the λ -Ursae Majorids (#524, LUM) well isolated (Fig. 10C). Results are in good agreement with Andreic et al. (2013).

The Southern λ -Draconids (#526, SLD), from Andreic et al. (2013), are a compact shower at the position as reported (Fig. 10D). Our measured semi-major axis of $a = 4.29 \pm 0.35$ AU is in good agreement with that reported before ($a = 4.0$ AU).

The η -Hydrids (#529, EHY) are a well-defined shower next to the strong sigma Hydrids (#16, HYD). First reported in a separate paper by Segon et al. (2013b) from SonotaCo and CMN data, CAMS results are in good agreement (Fig. 11A). Kornos et al. (2014) assigned 18 meteors from the independent EDMOND database.

The η -Corvids (#530, ECV) were first found by Molau et al. (2013) from single-station video observations. In good agreement, the CAMS survey detects a grouping at this position (Fig. 11B). The measured speed of 68.1 ± 0.2 km/s is slightly lower than that reported before (69.4 km/s). Kornos et al. (2014) assigned 6 meteors from EDMOND.

The γ -Aquilids (#531, GAQ) are a diffuse concentration of radiants in a strong sporadic background (Fig. 11C). Segon et al. (2014a) reported peak activity at $\lambda_o = 45^\circ$, but we have activity centered at 58° during an activity period $\lambda_o = 46\text{--}64^\circ$.

The July ξ -Arietids (#533, JXA) were reported by Segon et al. (2014a), having a mean orbit similar to Comet C/1964 N1 (Ikeya). CAMS results for this long-period shower are in good agreement (Fig. 11D). Kornos et al. (2014) tentatively detected this shower from EDMOND data.

The 49-Andromedids (#549, FAN) are well separated from the Perseids in the period $\lambda_o = 104\text{--}125^\circ$ (Fig. 12A). The shower was first reported by Andreic et al. (2014b). Also shown are the ζ -Cassiopeiids (#444, ZCS) (Segon et al., 2012), and the established c Andromedids (#411, CAN). At later times, the 49-Andromedids continue to be active, possibly as late as $\lambda_o = 141^\circ$, but the shower is more difficult to discriminate from the strong Perseids at that time. We chose to correct the radiant drift to $\lambda_o = 112^\circ$, but the median orbital elements include those extracted later as well. As a result, there is a wider discrepancy than usual between the reported solar longitude (our choice) and node (median value of the extracted sample).

The October γ -Camelopardalids (#555, OCP) are from Andreic et al. (2014b) and are shown in Fig. 12B. This is a diffuse high-declination shower, but well isolated from the sporadic background.

The December ω -Ursae Majorids (#563, DOU) are shown in Fig. 12C. Our results for radiant and entry speed agree with the results by Andreic et al. (2014b) from combined SonotaCo and Croatian Meteor Network data.

Andreic et al. (2014b) also identified the ξ -Hydrids (#567, XHY). CAMS results are in good agreement (Fig. 12D).

The o-Hydrids (#569, OHY) are active later from a nearby radiant position (Fig. 13A). We find a peak 3 days later than reported by Andreic et al. (2014b).

The February b-Herculids (#570, FBH) of Andreic et al. (2014b) are a diffuse shower in the toroidal ring on the daytime side of the apex source (Fig. 13B).

4. Discussion

4.1. Extraction of showers

The criterion most useful for isolating the showers from the sporadic background was D_h (Jopek, 1993). Not surprisingly, we found that the most suitable D_h threshold value depended on the type of shower under consideration and the orbital element distribution of the local sporadic background. The median threshold value for Jupiter Family comet type orbits was $D_h = 0.10$, while Halley-type and long-period comet sources required $D_h = 0.15$, but individual choices ranged from $D_h = 0.06$ – 0.25 .

The choice of the threshold value was based on what value best identified all meteors within a visible cluster in both radiant and Π - i diagrams. Our attempt to find a more formal approach to define the threshold value was thwarted by the erratic nature of the background orbital element distribution. Galligan (2003) established D_D cutoffs as a function of inclination that defined what fraction of a shower was recovered from the sporadic background. In his case, however, the sporadic background dominated the radar observations. The interactive approach of changing the threshold value on a case-by-case basis always seemed to extract a cluster more cleanly from the sporadic background in our data.

Note that the published definition of the D_n criterion has an error. Eq. (20) in Valsecchi et al. (1999), used to compute the components of U , should read $-\lambda$ and $-\varepsilon$. For the reference plane to coincide with the ecliptic plane, the rotation must be by $-\varepsilon$, not by ε , and for the Sun to be on the negative x -axis, the other rotation must be by $-\lambda$, not λ . The published equations used the anti-clock rotation direction for the rotation matrices. This was corrected in the CAMS StreamFinder application.

4.2. Duplicates and none-detections

Duplications have crept into the Working List, mainly because the same shower is detected at different times in the year. When viewed in Sun-centered ecliptic coordinates, these showers coincide. This is perhaps a better criterion to recognize duplicates than for a shower to have similar orbital elements (Andreic et al., 2014a). The list of Andreic et al. includes, for example, the Northern and Southern Taurids as having similar orbital elements.

Based on their overlap in Sun-centered ecliptic coordinates, the following showers are likely duplicates. The later addition should be removed from the Working List: The ζ -Draconids (#73) are the κ -Cygnids (#12), the ν -Draconids (#220) are the August Draconids (#197), the January Comae Berenicids (#90) are the Comae Berenicids (#20), and the Southern σ -Sagittariids (#168) are the Southern μ -Sagittariids (#69). The ξ -Aurigids (#205) are part of the Perseids (#7). The ζ -Taurids (#226) are part of the Orionids (#8). The October ι -Cassiopeiids (#230) are the Leonis Minorids (#22), also pointed out by Andreic et al. (2014a). The November μ -Arietids (#249) are the Andromedids (#18), and the before mentioned ν -Cygnids (#409) are the ζ -Cygnids (#40).

Because the showers up to #318 were originally reported based mostly on small numbers of photographed meteoroid orbits, a non-detection in this CAMS data can be justified reason to dismiss the shower from the Working List. We therefore recommend removal because they are not detected while they should have been: showers ##34, 43, 46, 92, 104, 125, 126, 127, 131, 133, 136, 139, 142, 147, 148, 150, 157, 167, 169, 193, 194, 199, 207, 210, 217, 218, 224, 228, 229, 231, 232, 234, 235, 236, 237, 241, 244, 245, 258, and 260. Based on this list, a few proposed complexes should also be removed from the Working List, namely the δ -Leonids Complex (#29) and the March Virginids Complex (#93).

For now, we recommend that the remaining showers be kept in the Working List, still in need of confirmation, mostly based on the possibility of weak ($S/B < 2$) activity in CAMS data. We also recommend that periodic showers known from past visual observations be kept in the list, because they may not have returned during the period of our CAMS observations: the γ -Delphinids (#65), the February Canis Majorids (#111), the α -Bootids (#138), the June Lyrids (#166) and the ε -Eridanids (#209). Similarly, we cannot provide evidence to dismiss southern hemisphere or daytime showers. Finally, validation of the remaining asteroidal streams (##263–289) requires further study, because most are based on (random?) pairs of slow-moving meteors and do not stand out as a cluster in the CAMS data, in part due to their low angular velocity.

The CMOR is particularly sensitive to 20–40 km/s meteors, but they need to be faint enough to create specular trails ($>+5$ magnitude). In this velocity range, CMOR observes mostly +6 to +8 magnitude meteors. Slower meteors generate too few electrons, while fast meteors ablate higher in the atmosphere where their generated electrons spread quickly (echo height ceiling effect). Because CAMS sees predominantly +4 to -2 magnitude meteors, some showers rich in faint meteors are not detected by CAMS, while many fast and very slow showers detected by CAMS are not seen by CMOR.

The second CMOR batch (Brown et al., 2010) contains some duplicates: the Microscopiids (#370) are the Piscis Austrinids (#183). The λ -Draconids (#383) may be the ξ -Draconids (#242). The ν -Geminids (#397) appear to be part of the November Orionids (#250). Also, the β -Camelopardalids (#365) appear to be the June μ -Cassiopeiids (#362), while the α -Pegasids (#367) may be the July β -Pegasids (#366).

Based on the fact that the Sun-centered ecliptic coordinates of the radiant overlap, the new reports of video-derived showers also contain some duplicates that should be removed from the Working List: The λ Ophiuchids (#460, LOP) are the ϕ -Ophiuchids (#412). The α -Triangulids (#414, ATR) are a late component of the ψ -Piscids (#372), while the August Piscids (#415, AUP) belong to the July Pegasids (#175). The η -Taurids (#417, ETT) are the χ -Taurids (#388). The θ -Piscids (#508, TPI) and August β -Piscids (#342, BPI) are the Northern δ -Aquiriids (#26), as also pointed out by Andreic et al. (2014a) and Molau and Kerr (2014). The ε -Virginids (#513, EPV) are the December δ -Virginids (#428), also pointed out by Andreic et al. (2014a). The α -Leonids (#515, OLE) are the December Canis Minorids (#253, CMI). The Southern α -Pegasids (#522, SAP) are the July Pegasids (#175), as noticed by Andreic et al. (2014a). The ν -Ursae Majorids (#527, UUM) are the November σ -Ursae Majorids (#488), also pointed out by Andreic et al. (2014a). The May λ -Draconids (#532, MLD) are the Camelopardalids (#451, CAM), as noticed by Andreic et al. (2014a), while the 15-Aquiriids (#548, FAQ) are part of the Northern June Aquiriids (#164, NZC).

CAMS validated only a small fraction of all recently added showers from video data. That is surprising, because the newly added showers are based on similar (but less complete) orbit surveys. We suspect that most of the unconfirmed showers are insignificant groupings of unrelated meteoroids. Only four of the recently added showers 548–572 by Andreic et al. (2014b) are confirmed, and none of the showers 573–596 by Gural et al. (2014) or showers 599–622 by Segon et al. (2014a,c) are detected in our analysis of CAMS data. These papers all use automated D -criterion based approaches with relatively liberal threshold values ($D_{sh} = 0.15$), which may have led to spurious detections, especially in the direction of the antihelion source. In the case of showers 432–443 by Shigeno and Yamamoto (2012), a few showers show some similarity to CAMS-detected showers, but only if the measured entry speed is wrong.

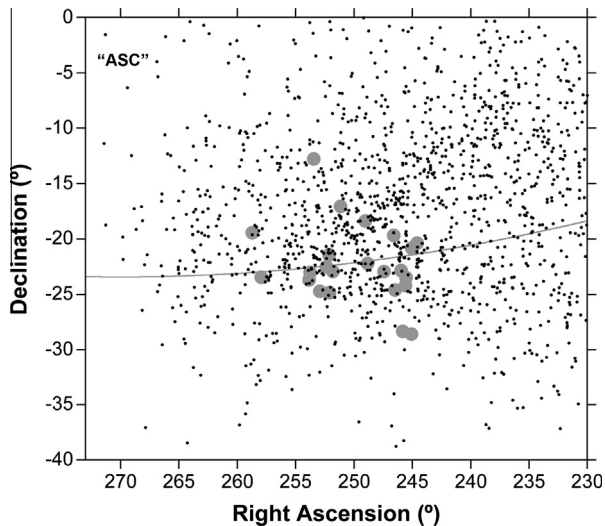


Fig. 14. α -Scorpiids (#55, ASC) – period $\lambda_0 = 42\text{--}62^\circ$. Gray dots mark the shower radiant reported in various literature sources from the compilation by Jenniskens (2006, pp. 706–707), just above and below the ecliptic plane (gray line). All are drift-corrected to $\lambda_0 = 55^\circ$.

From the early Harvard shower list, NOT detecting the α -Scorpiids (#55, ASC) is remarkable, because many authors have reported isolating the α -Scorpiids from photographed orbit surveys (for a compilation see Jenniskens, 2006). Fig. 14 gathers these previously reported radiant positions, all drift-corrected to $\lambda_0 = 55^\circ$. It is not a good sign that these reported positions scatter widely across the antihelion source during the solar longitude interval $\lambda_0 = 42\text{--}62^\circ$, covering the time of peak activity reported by the various authors. The antihelion source is strong during this time interval and the radiant map may have some structure to it, but not enough, yet, to isolate a group that likely originated from the same parent body.

5. Conclusions

CAMS set out to validate as many as possible of the 486 meteor showers in the IAU Working List on Meteor Showers that needed confirmation. After the first 2.5 years of observations, the database of $\sim 110,000$ measured meteoroid trajectories was searched for surface density enhancements in maps of the drift-corrected Sun-centered ecliptic radiant coordinates at positions of previously reported meteor showers. In this paper, we confirm that 41 of these showers do exist, adding to the 31 previously confirmed showers. The newly confirmed showers can now also be moved to the IAU List of Established Showers.

A number of duplicates in the current Working List are identified based on the showers having the same Sun-centered ecliptic coordinates of the radiant.

Where previous records are based on too few meteors, recommendations are made to remove showers from the Working List on grounds that they could not be detected in more extensive data.

Only few of the recently reported video-derived showers are validated, which were extracted with automatically linked *D*-criterion algorithms using weak thresholds. Isolating similar orbits from a database in these cases may not mean they originated from the same parent body. Based on the CAMS data, it is difficult to make recommendations for removal, because showers may be irregular in activity. At least some have tentative detections in CAMS data.

Future improvement of our understanding of meteoroid streams at Earth will come from ongoing CAMS operations and

its expansion to the southern hemisphere. Theoretical modeling is needed to establish the proposed links with parent body Near Earth Objects listed in the tables, and to interpret the showers and the sporadic background as a record of past parent body evolution.

Acknowledgments

We thank all CAMS team members for their support of the project: amateur astronomers and students who helped build CAMS hardware, supported CAMS operations over the years, and assisted in the ongoing data reduction effort. Fremont Peak State Park and Lick Observatory generously hosted the deployment of the CAMS camera stations. The CAMS project was made possible by grants from NASA's Planetary Astronomy (NNX08AO64G) and Near Earth Object Observation (NNX12AM14G) programs.

References

- Andreic, Z. et al., 2013. Ten possible new showers from the Croatian Meteor Network and SonotaCo datasets. *J. Int. Meteor. Org.* 41, 103–108.
- Andreic, Z., Segon, D., Vida, D., 2014a. A statistical walk through the IAU MDC database. In: Rault, J.-L., Roggemans, P. (Eds.), Proceedings of the International Meteor Conference, Giron, France, 18–21 September 2014. International Meteor Organization, pp. 126–133.
- Andreic, Z. et al., 2014b. Results of CMN 2013 search for new showers across CMN and SonotaCo databases I. *J. Int. Meteor. Org.* 42, 90–97.
- Brown, P. et al., 2008a. A meteoroid stream survey using the Canadian Meteor Orbit Radar – I: Methodology and radiant catalogue. *Icarus* 195, 317–339.
- Brown, P. et al., 2008b. The Canadian Meteor Orbit Radar meteor stream catalogue. *Earth, Moon, Planets* 102, 209–219.
- Brown, P. et al., 2010. A meteoroid stream survey using the Canadian Meteor Orbit Radar – II: Identification of minor showers using a 3D wavelet transform. *Icarus* 207, 66–81.
- Cook, A.F. et al., 1972. Yet another stream search among 2401 photographic meteors. *Smith. Contrib. Astrophys.* 15, 1–5.
- Drummond, J.D., 1981. A test of comet and meteor shower associations. *Icarus* 45, 545–553.
- Galligan, D., 2003. Radar meteoroid orbit stream searches using cluster analysis. *Mon. Not. R. Astron. Soc.* 340, 899–907.
- Greaves, J., 2012. Four IAU MDC working list meteor showers confirmed via SonotaCo Network. *J. Int. Meteor. Org.* 40, 53–58.
- Gural, P.S., 2012. A new method of meteor trajectory determination applied to multiple unsynchronized video cameras. *Meteorit. Planet. Sci.* 47, 1405–1418.
- Gural, P.S. et al., 2014. Results of CMN 2013 search for new showers across CMN and SonotaCo databases II. *J. Int. Meteor. Org.* 42, 132–138.
- Holman, D., Jenniskens, P., 2012a. Confirmation of the Northern Delta Aquariids (NDA, IAU #26) and the Northern June Aquilids (NZC, IAU #164). *J. Int. Meteor. Org.* 40, 166–170.
- Holman, D., Jenniskens, P., 2012b. Confirmation of the July Gamma Draconids (GDR, IAU #184). *J. Int. Meteor. Org.* 40, 36–41.
- Holman, D., Jenniskens, P., 2013. Discovery of the Upsilon Andromedids (UAN, IAU #507). *J. Int. Meteor. Org.* 41, 43–47.
- Jacchia, L.G., Verniani, F., Briggs, R.E., 1961. An analysis of the atmospheric trajectories of 413 precisely reduced photographic meteors. *Smiths. Contrib. Astrophys.* 10, 1–45.
- Jenniskens, P., 2006. Meteor Showers and their Parent Comets. Cambridge University Press, Cambridge, UK, 790pp.
- Jenniskens, P., 2008. Meteoroid streams that trace to candidate dormant comets. *Icarus* 194, 13–22.
- Jenniskens, P., 2012. Mapping meteoroid orbits. *Sky Telescope* 87, 20–25.
- Jenniskens, P., Gural, P.S., 2011. Discovery of the February η -Draconids (FED, IAU#427): The dust trail of a potentially hazardous long-period comet. *J. Int. Meteor. Org.* 39, 93–97.
- Jenniskens, P., Haberman, B., 2013. “Thatcher's Ghost”: Confirmation of the ν -Cygnids (NCY, IAU #409). *J. Int. Meteor. Org.* 41, 75–76.
- Jenniskens, P. et al., 2009. On how to report new meteor showers. *J. Int. Meteor. Org.* 37, 19–20.
- Jenniskens, P. et al., 2011. CAMS: Cameras for Allsky Meteor Surveillance to establish minor meteor showers. *Icarus* 216, 40–61.
- Jenniskens, P., Gural, P.S., Holman, D., 2012. The established meteor showers as seen in video meteoroid orbit surveys. In: Gyssens, M., Roggemans, P. (Eds.), Proceedings of the International Meteor Conference, La Palma, 20–23 September 2012. The International Meteor Organization, Belgium, pp. 38–43.
- Jenniskens, P. et al., 2016. The established meteor showers as observed by CAMS. *Icarus* 266, 331–354.
- Jopek, T.J., 1993. Remarks on the meteor orbital similarity *D*-criterion. *Icarus* 106, 603–607.
- Jopek, T.J., Kanuchová, Z., 2014. Current status of the IAU MDC meteor shower database. In: Jopek, T.J., Rietmeijer, F.J.M., Watanabe, J., Williams, I.P. (Eds.),

- Meteoroids 2013, Proc. of the Astron. Conf. held at A.M. University, Poznan, Poland, August 26–30, 2013. A.M. University Press, pp. 353–364.
- Jopek, T.J., Rudawska, R., Pretka-Ziomek, H., 2006. Calculation of the mean orbit of a meteoroid stream. *Mon. Not. R. Astron. Soc.* 371, 1367–1372 (erratum: 2008, *Mon. Not. R. Astron. Soc.* 387, 1741).
- Jopek, T.J., Rudawska, R., Bartczak, P., 2008. Meteoroid stream searching: The use of the vectorial elements. *Earth, Moon, Planets* 102, 73–78.
- Kanamori, T., 2009. A meteor shower catalog based on video observations in 2007–2008. *WGN, J. Int. Meteor. Org.* 37, 55–62.
- Korlevic, K. et al., 2013. Croatian Meteor Network catalogues of orbits for 2008 and 2009. *J. Int. Meteor. Org.* 41, 48–51.
- Kornos, L. et al., 2012. Database of meteoroid orbits from several European video networks. In: Gyssens, M., Roggemans, P. (Eds.), Proceedings of the International Meteor Conference, La Palma, 20–23 September 2012. The International Meteor Organization, Belgium, pp. 21–25.
- Kornos, L. et al., 2014. Confirmation and characterization of IAU temporary meteor showers in EDMOND database. In: Jopek, T.J., Rietmeijer, F.J.M., Watanabe, J., Williams, I.P. (Eds.), Meteoroids 2013, Proc. Astron. Conf. held at A.M. University, Poznan, Poland, August 26–30, 2013. A.M. University Press, pp. 225–233.
- Koukal, J. et al., 2014. Some interesting meteor showers in EDMOND database. *J. Int. Meteor. Org.* 42, 7–13.
- Lindblad, B.A., 1971a. A stream search among 865 precise photographic meteor orbits. *Smiths. Contrib. Astrophys.* 12, 1–13.
- Lindblad, B.A., 1971b. 2. A computerized stream search among 2401 photographic meteor orbits. *Smiths. Contrib. Astrophys.* 12, 14–24.
- Molau, S., Arlt, R., 1997. Meteor shower radiant positions and structures as determined from single station video observations. *Planet. Space Sci.* 45, 857–864.
- Molau, S., Barentsen, G., 2014. Status and history of the IMO Video Meteor Network. In: Jopek, T.J., Rietmeijer, F.J.M., Watanabe, J., Williams, I.P. (Eds.), Meteoroids 2013, Proc. Astron. Conf. held at A.M. University, Poznan, Poland, August 26–30, 2013. A.M. University Press, pp. 297–305.
- Molau, S., Kac, J., 2009. Results of the Video Meteor Network – March 2009. *J. Int. Meteor. Org.* 37, 92–93.
- Molau, S., Kerr, S., 2014. Meteor showers of the southern hemisphere. *J. Int. Meteor. Org.* 42, 68–75.
- Molau, S., Rendtel, J., 2009. A comprehensive list of meteor showers obtained from 10 years of observations with the IMO Video Meteor Network. *J. Int. Meteor. Org.* 37, 98–121.
- Molau, S. et al., 2013. Results of the IMO Video Meteor Network – January 2013. *J. Int. Meteor. Org.* 41, 61–66.
- Nilsson, C.S., 1964. A southern hemisphere radio survey of meteor streams. *Astr. J. Phys.* 17, 205–256.
- Phillips, M., Jenniskens, P., Grigsby, B., 2011. Confirmation of the April ρ -Cygnids (ARC, IAU #348). *J. Int. Meteor. Org.* 39, 131–136.
- Rudawska, R., Jenniskens, P., 2014. New meteor showers identified in the CAMS and SonotaCo meteoroid orbit surveys. In: Jopek, T.J., Rietmeijer, F.J.M., Watanabe, J., Williams, I.P. (Eds.), Meteoroids 2013, Proc. Astron. Conf. held at A.M. University, Poznan, Poland, August 26–30, 2013. A.M. University Press, pp. 217–224.
- Segon, D. et al., 2012. New shower in Cassiopeia. *J. Int. Meteor. Org.* 40, 195–200.
- Segon, D. et al., 2013a. 8 new showers from Croatian Meteor Network data. *J. Int. Meteor. Org.* 41, 70–74.
- Segon, D. et al., 2013b. A possible new meteor shower – η Hydrids. *J. Int. Meteor. Org.* 41, 157–159.
- Segon, D. et al., 2014a. New showers from parent body search across several video meteor databases. *J. Int. Meteor. Org.* 42, 57–64.
- Segon, D. et al., 2014b. A possible new shower on Eridanus–Orion border. *J. Int. Meteor. Org.* 42, 218–221.
- Segon, D. et al., 2014c. A parent body search across several video meteor data bases. In: Jopek, T.J., Rietmeijer, F.J.M., Watanabe, J., Williams, I.P. (Eds.), Meteoroids 2013, Proc. of the Astron. Conf. held at A.M. University, Poznan, Poland, August 26–30, 2013. A.M. University Press, pp. 251–262.
- Sekanina, Z., 1973. Statistical model of meteor streams. III – Stream search among 19,303 radio meteors. *Icarus* 18, 253–284.
- Sekanina, Z., 1976. Statistical model of meteor streams. IV – A study of radio streams from the synoptic year. *Icarus* 27, 265–321.
- Shigeno, Y., Yamamoto, M., 2012. Meteor shower catalog based on 3770 triangulation analyses of double-station image-intensified video observations over Japan. *J. Int. Meteor. Org.* 40, 24–35.
- Southworth, R.B., Hawkins, G.S., 1963. Statistics of meteor streams. *Smithson. Contrib. Astrophys.* 7, 261–285.
- Terentjeva, A.K., 1989. Fireball streams. *J. Int. Meteor. Org.* 17, 242–245.
- Valsecchi, G.B., Jopek, T.J., Froeschle, Cl., 1999. Meteoroid stream identification: A new approach – I. Theory. *Mon. Not. R. Astron. Soc.* 304, 743–750.
- Vida, D. et al., 2012. Possible new meteor shower detected from CMN and SonotaCo data. In: Gyssens, M., Roggemans, P. (Eds.), Proceedings of the International Meteor Conference, La Palma, 20–23 September 2012. The International Meteor Organization, Belgium, pp. 31–33.